HHS Public Access

Author manuscript

J Med Chem. Author manuscript; available in PMC 2015 October 14.

Published in final edited form as:

J Med Chem. 2015 March 26; 58(6): 2746–2763. doi:10.1021/jm501929n.

Development of Novel ACK1/TNK2 Inhibitors Using a Fragment-Based Approach

Harshani R. Lawrence[*,†,‡,§], **Kiran Mahajan**[†,§], **Yunting Luo**[‡], **Daniel Zhang**[†], **Nathan Tindall**[†], **Miles Huseyin**[†], **Harsukh Gevariya**[†], **Sakib Kazi**[†], **Sevil Ozcan**[†], **Nupam P. Mahajan**[*,†,§], and **Nicholas J. Lawrence**[*,†,§]

[†]Drug Discovery Department, Moffitt Cancer Center, 12902 Magnolia Drive, Tampa, Florida 33612, United States

[‡]Chemical Biology Core, Moffitt Cancer Center, 12902 Magnolia Drive, Tampa, Florida 33612, United States

[§]Department of Oncologic Sciences, University of South Florida, Tampa, Florida 33620, United States

Abstract

The tyrosine kinase ACK1, a critical signal transducer regulating survival of hormone-refractory cancers, is an important therapeutic target, for which there are no selective inhibitors in clinical trials to date. This work reports the discovery of novel and potent inhibitors for ACK1 tyrosine kinase (also known as TNK2) using an innovative fragment-based approach. Focused libraries were designed and synthesized by selecting fragments from reported ACK inhibitors to create hybrid structures in a mix and match process. The hybrid library was screened by enzyme-linked immunosorbent assay-based kinase inhibition and ^{33}P HotSpot assays. Systematic structure–activity relationship studies led to the identification of compound (*R*)-**9b**, which shows potent in vitro (IC_{50} = 56 nM, n = 3, ^{33}P HotSpot assay) and in vivo (IC_{50} < 2 μM, human cancer cell lines) ACK1 inhibition. Both (*R*)-**9b** and (*S*)-**9b** were stable in human plasma and displayed a long half-life ($t_{1/2}$ > 6 h).

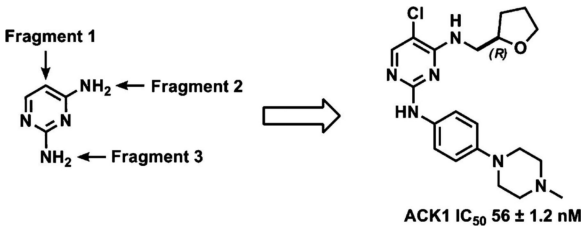

[*]**Corresponding Authors**Harshani.Lawrence@moffitt.org. Phone: (813) 745-6076. Fax: (813) 745-6748. Nupam.Mahajan@moffitt.org. Phone: (813) 745-4078. Fax: (813) 745-6748. Nicholas.Lawrence@moffitt.org. Phone: (813) 745-6037. Fax: (813) 745-6748..

Supporting Information

Synthetic protocols for preparation of sulfides **10a–d**, sulfones **11a–d**, sulfides and sulfones **12a–r**, and compounds **23–42** and Figures S1 and S2 showing (*R*)-**9b** superposed in JAK2 and ALK. This material is available free of charge via the Internet at http://pubs.acs.org.

H.R.L., K.M., N.P.M. and N.J.L. are named as inventors on US patent application 60/862,763 titled “Inhibitors of ACK1/TNK2 Tyrosine Kinase.”

INTRODUCTION

The ACK1 tyrosine kinase is aberrantly activated, amplified, or mutated in many types of human cancers, including prostate, breast, pancreatic, ovarian, and lung cancers.[1,2] Aberrantly activated ACK1 drives cell growth via a number of molecular mechanisms, which we have recently reviewed.[3] Several recent discoveries underscore its tumor-promoting functions. For example, ACK1 phosphorylates the androgen receptor, at Tyr267 in its transactivation domain, in an androgen-independent manner to promote castration-resistant prostate cancer (CRPC) growth.[4,5] ACK1 has been shown to promote prostate tumorogenesis by phosphorylating the WW domain-containing oxidoreductase (Wwox) tumor suppressor[6] on Tyr287, leading to its polyubiquitination and subsequent degradation in prostate cancer models.[7] We have also shown that ACK1 phosphorylates and activates the key signaling kinase AKT at Tyr176,[8] which plays important roles in human physiology and disease.[9–11] When AKT is phosphorylated on Tyr176 by ACK1, it functionally participates in the progression of breast cancer by suppressing proapoptotic pathways.[8] Mechanistically, phosphorylation on AKT Tyr176 by ACK1 activates PI3K-independent AKT activation and facilitates the survival of breast cancer cells by suppressing proapoptotic pathways.[8] Conversely, knockdown of ACK1 expression by siRNA suppressed AKT Tyr176 phosphorylation and activation in breast, prostate, and pancreatic cancer cells and increased expression of proapoptotic genes such as Bim and Fas.[8,12] Recently, ACK1 has also been shown to phosphorylate histone demethylase KDM3A (JHDM2A) at Tyr1114 in breast cancer cells, conferring tamoxifen resistance.[13]

The importance of ACK1 activation in tumor initiation in vivo first became evident when we generated transgenic mice expressing ACK1 specifically in the prostate. These ACK1 transgenic mice developed PIN, indicating that its activation is crucial in early stages of tumor initiation.[8] Collective evidence in preclinical models therefore validates ACK1 as an important target for anticancer drugs and has driven the development of ACK1 inhibitors.[1]

Selected examples of ACK1 inhibitors are shown in Figure 1. A series of 4-amino-5,6-biarylfuro[2,3-*d*]pyrimidines (structures **1a–1c**, Figure 1) were found to inhibit ACK1 and the related member of the src kinase family Lck (lymphocyte-specific kinase).[14,15] For example, compound **1a** potently inhibits both ACK1 and Lck and was useful in the development of further compounds for the treatment of T cell-mediated autoimmune and inflammatory disease as a consequence of Lck inhibition. We used compound **1b** (AIM-100) as a chemical probe for ACK1 inhibition, since it was reported to inhibit Lck to a lesser extent (ACK1:Lck = 5:1) than **1a** (Lck:ACK1 = 1.8:1). We have shown that AIM-100 inhibits ACK1-dependent AKT Tyr176[12] in pancreatic cancer cells and AR Tyr267[16] phosphorylation. AIM-100 also inhibits castration and radioresistant prostate xenograft tumor growth via inhibition of AR Tyr267 phosphorylation.[5] A study of further members of the 4-amino-5,6-biarylfuro[2,3-*d*]pyrimidine series showed that the dithiolane **1c** was an exceptionally potent ACK1 inhibitor (K_i = 0.3 nM). This compound inhibits the growth of an ACK1-dependent cell line with an IC_{50} of 5 nM. However, its poor pharmacokinetic properties (attributed to oxidation of both the dithiolane ring and NMe_2) precluded further development. A series of pyrazolopyrimidines of type **2** have also been developed by Amgen as ACK1 inhibitors.[17] For example, compound **2a** potently inhibits ACK1 in vitro

(IC_{50} = 2 nM) and in intact cells, as measured by inhibition of ACK1 autophosphorylation (IC_{50} = 20 nM). Gray and co-workers have identified the ACK1 inhibitor **3** by high-throughput kinase profiling of a focused library of pyrimidodiazepines.[18] This compound abolishes EGF-induced ACK1 autophosphorylation (Tyr284) in HEK293 cells at concentrations of 2 μM. It also inhibits A549 lung cancer cell growth at 10 μM. A series of imidazopyrazine-based ACK1 inhibitors have been developed by Jin and co-workers at OSI/Astellas.[19] For example, compound **4** is a potent and orally bioavailable ACK1 inhibitor in mouse models and possesses good experimental ADMET (absorption, distribution, metabolism, elimination, and toxicity) properties. Compound **4** inhibits ACK1-mediated phosphorylation of poly(GT) in an AlphaScreen assay with an IC_{50} of 110 nM. Moreover, it potently inhibits ACK1 in a cellular context. In NCI-H1703 human non-small-cell lung cancer cells, its IC_{50} for ACK1 inhibition is 35 nM as measured by an ELISA assay.[19]

Several promiscuous kinase inhibitors have been shown to inhibit ACK1. For example, the Src/Abl kinase inhibitor bosutinib[20] inhibits ACK1 with an IC_{50} of 2.7 nM.[21] Bosutinib was found to inhibit cell migration and invasion but not cell viability in a panel of non-small-cell lung cancer (NSCLC) cell lines.[22] These effects were not seen when ACK1 was knocked-down specifically in K-Ras mutant cell lines. Dasatinib, another BCR/Abl and Src family tyrosine kinase inhibitor, inhibits ACK1 with a K_D of 6 nM.[23] Dasatinib was shown to inhibit both ACK1 autophosphorylation and AR phosphorylation of Tyr-267 in heregulin-stimulated human prostate cancer LNCaP cells with IC_{50} values of <5 nM.[24] Additionally, dasatinib significantly reduced the growth of LNCaP cells expressing constitutively activated ACK1 in a mouse xenograft model.[24] Chemical and phosphoproteomic approaches revealed ACK1 to be a target of dasatinib in human lung cancer cells.[25]

In this paper, we describe the development of novel ACK1 inhibitors by analysis of known ACK1 inhibitors, including **1b** (AIM-100, Figure 2B), the pyrazolopyrimidine derivative **2b**[17] (Figure 2A), and the ALK inhibitor **5** (TAE684[26] (Figure 2C) (which strongly cross-inhibits ACK1 from published inhibitor profiling data sets; K_d = 2 nM[27] and K_i = 1 nM[28]). The binding modes of the three inhibitors are shown in Figure 2, as derived from the X-ray structure of **2b** with ACK1[17] (PDB 3EQR), **1b** (AIM-100) modeled using the X-ray structure of an analogue with ACK1[29] (PDB 4EWH), and **5** modeled using its X-ray structure with ALK[30] (PDB 2XB7). These inhibitors bind the ACK1 hinge residue Ala208 via the pyrimidyl group, positioning groups in the hydrophobic pocket beyond the gatekeeper and in the ribose binding region.[26] The bisanilinopyrimidine scaffold has long been recognized as a classical kinase inhibitor motif.[2,13,31] Recently, we reported our efforts in identifying novel and exceptionally potent Aurora A inhibitors using the bisanilinopyrimidine scaffold.[32,33] In the development of novel ACK1 inhibitors, our design process incorporated an aminopyrimidine structure as the hinge binding group (Figure 2D) and fragments of **1b**, **2b**, and **5** as R^1, R^2, and R^3 (Figure 2D) groups to create hybrid structures in a mix and match process (Figure 2).

CHEMISTRY

Synthesis of (±)-9a–t as ACK1 Inhibitors

First, the synthesis of compounds (±)-**9a–t** with R^1, R^2, and R^3 groups was achieved from a set of 2,4-dichloropyrimidine building blocks, **7** (Scheme 1), by sequential reactions with two amine fragments. The starting materials **7a–e** reacted with (±)-tetrahydrofurfurylamine using method a (Scheme 1) to obtain the intermediates (±)-**8a–e**, which were subsequently reacted with the requisite anilines R^3NH_2 (Scheme 1) using method b to obtain the final compounds (±)-**9a–t** with A- and B-rings (Scheme 1). The synthesis of building block **7c** was achieved from readily available dihydroxypyrimidine-5-carboxylic acid via dichloropyrimidine-5-carbonyl chloride[31] as shown in Scheme 2 in good yield.

Synthesis of the Sulfones 12a–j and Sulfides 12k–r as ACK1 Inhibitors

The synthesis of sulfone-substituted derivatives **12a–j** was undertaken from **7c** as shown in Scheme 2. Our attempts to synthesize sulfone derivatives **11** by direct reaction of **7c** with *o*-(sulfonylalkyl)aniline using microwave heating conditions (100–170 °C, 30 min, ethanol, THF, or dioxane) or conventional alkylation conditions (sodium hydride in DMF or THF at room temperature followed by heating) were unsuccessful. Therefore, we first generated the sulfide intermediates **10** by reacting building block **7c** with appropriate aniline sulfides (method a, Scheme 2), which were then oxidized to sulfone intermediates **11** using *m*CPBA (method b, Scheme 2). The intermediates **10** (Scheme 2) were used to prepare the final sulfide analogues **12k–r** with the B-ring (see the Supporting Information). The B-ring in these analogues was introduced using microwave heating in HCl (4 M in dioxane) (method c, Scheme 2) to successfully obtain the final compounds in good yields with >95% purity as determined by HPLC.

Synthesis of Enantiomers of 9b

The synthesis of (*R*)-**9b** and (*S*)-**9b** stereoisomers was achieved as shown in Scheme 3 from commercially available (*R*)- and (*S*)-tetrahydrofurfurylamines. The optical rotations ($[\alpha]_D$) of commercially available (*S*)-(+)-tetrahydrofurfurylamine and (*R*)-(–)-tetrahydrofurfurylamine were measured as +11.85 and –11.33, respectively, and are in agreement with the reported optical rotation of the (*S*)- and (*R*)-stereoisomers, +12 and –12, respectively.[34] We were able to resolve the enantiomers of (±)-**9b** using chiral HPLC (see the Experimental Section) and to determine the enantiomeric purity of (*R*)-**9b** and (*S*)-**9b** using chiral HPLC as >98%.

RESULTS AND DISCUSSION

Analogue Design and in Vitro Structure–Activity Relationship (SAR)

The ability of the pyrimidines **9** and **12** to inhibit ACK1 kinase activity was first examined using a novel ELISA (enzyme-linked immunosorbent assay) developed in our laboratory.[8] This assay measured the ability of ACK1 to specifically phosphorylate a tyrosine residue in a peptide derived from AKT (of sequence ATGRYYAMKIL)[8] followed by detection of phosphorylation by an antibody-based approach.[8] Loss of ACK1 kinase activity was directly proportional to decreased phosphorylation of AKT peptide. Subsequently, IC_{50} values for

those compounds that inhibited ACK1 activity by >80% at a concentration of 10 μM in the ELISA were determined in a ^{33}P HotSpot assay (Reaction Biology). In the present work, we performed SAR studies using the ELISA (see the Experimental Section) and dose response data obtained from the ^{33}P HotSpot assay. The (±)-tetrahydrofurfurylamine fragment (Figure 2B) from **1b** was incorporated into the design and synthesis of compounds **9a–t** (i.e., R^2 group, Scheme 1) as a racemic mixture with >95% purity as determined by HPLC. The R^1 substituents at the 5-position of the pyrimidine and R^3 aniline fragments (Scheme 1 and Figure 2D) in compounds **9a–t** were chosen from **2b** (Figure 2A) and **5** (Figure 2C). The R^3 aniline building blocks shown in Scheme 1 were chosen to aid inhibitor binding interactions as well as to modulate the druglike properties such as solubility, hydrophobicity (cLogP < 5), cell permeability, and polar surface area (<140 Å). We incorporated anilines possessing polar hydrophilic groups (or water-solubilizing groups such as morpholine, piperazine, and piperidine) as R^3.

Our initial SAR from compounds **9a–t** (Scheme 1) indicated that Cl, Br, and 2-chloro-6-fluorocarboxamide groups in the 5-position of the pyrimidine ring (i.e., R^1) are important for ACK1 inhibitory activities, while methyl and F groups are unfavorable. This observation is consistent with the members of the set **9a–t**. For example, compounds **13** (76%, entry 3, Table 1) and **14** (66%, entry 4, Table 1) with Br and 2-chloro-6-fluorocarboxamide, respectively, as R^1 and *m*-fluoro-*p*-hydroxyaniline as R^3 showed improved ACK1 inhibition compared to the corresponding F and Me analogues **9t** (41% at 10 μM) and **9u** (49%) (entries 1 and 2, Table 1). Similarly, compounds **15** (65%), **16** (83%), and **9r** (85%), which contain Cl, Br, and 2-chloro-6-fluorocarboxamide fragments in the 5-position (entries 5–7, Table 1), respectively, and *p*-hydroxyaniline as R^3 showed 2–10-fold improvement in ACK1 inhibition compared to analogues with F (41%) and methyl (8%) as R^1 (not shown in Table 1; see the Supporting Information for synthesis). The related compounds **18** and **9q** (entries 9 and 10, Table 1) with hydrophobic methoxyaniline as R^3 showed moderate ACK1 inhibition of 67% and 68%, respectively, indicating hydrophilic anilines as R^3 are beneficial to maintain the in vitro ACK1 inhibitory activities.

The synthesis of sulfones **12a–j** (Scheme 2) was also undertaken in parallel on the basis of the initial SAR information available from compounds **9a–t** (Scheme 1). We used the building block **7c** as the starting point, in which a 2-chloro-6-fluorocarboxamide group occupies the 5-position of the pyrimidine ring (similar to the R^1 group in compounds **9a–t**) and later introduced sulfonyl-substituted anilines as R^2 (A-ring, Scheme 2), similar to the isopropylsulfonamide-containing A-ring of **5** (Figure 2C). Hydrophilic groups such as *p*-hydroxyaniline were introduced as the B-ring (Scheme 2). However, all the analogues from the set of sulfones **12a–j** showed weak ACK1 inhibition (<60% at 10 μM in the ELISA), and the sulfides **12k–r** generated using intermediate **10** (Scheme 2) showed very little ACK1 inhibitory activity in the ELISA (see the Supporting Information). Therefore, subsequent synthetic chemistry was predominantly focused on building blocks that contain Cl, Br, or 2-chloro-6-fluorocarboxamide as R^1 (**8a**, **8b**, and **8c**, Scheme 1) while keeping the (±)-tetrahydrofurfurylamine group as R^2.

Next, we further modified the R^3 group of **9** using the anilines shown in Scheme 1 while keeping R^1 as Cl, Br, or a 2-chloro-6-fluorocarboxamide group. Compounds **9c**, **9h**, and **9n**,

which contain *p*-morpholinoaniline fragments (entries 11–13, Table 1) as R^3 and Cl, Br, and 2-chloro-6-fluorocarboxamide groups as R^1, showed improved ACK1 inhibitory activities with IC_{50} values of 67.5, 106, and 48 nM, respectively, compared to earlier analogues, and this observation further suggests aniline fragments with hydrophilic/water-solubilizing moieties are well tolerated in the R^3 binding region. Compounds **9a**, **9i**, and **9m** with *p*-piperazinylaniline as R^3 also showed excellent ACK1 inhibitory activities (entries 14–16, Table 1) with IC_{50} values of 81, 94, and 33 nM, respectively, similar to morpholine analogues, further suggesting anilines with hydrophilic groups as R^3 have a positive effect on the ACK1 inhibition. As expected, compounds **9b**, **19**, and **20** with (methylpiperazinyl)aniline as R^3 (entries 17–19, Table 1) showed high ACK1 inhibitory activities with IC_{50} values of 54, 48, and 48 nM, respectively. Compound **9s** (entry 26, Table 1) with piperidinecarboxylic acid showed a significantly improved ACK1 inhibitory activity with an IC_{50} value of 34 nM, compared to its related Cl and Br analogues **9e** and **9j**, respectively (entries 24 and 25, Table 1). Interestingly, substitution of the *N*-methyl group of compound **20** (entry 19, Table 1) with a succinyl amide group as in compound **22** (entry 27, Table 1) led to >1.5-fold improvement in ACK1 inhibitory activity with an IC_{50} of 28 nM. We noticed that compounds **9e**, **9s**, and **22** (entries 24, 26, and 27, Table 1) with a carboxylic acid group as the H-bond donor/acceptor overall improved ACK1 inhibitory activities, indicating its potential as a handle, for example, in amide synthesis, for further SAR exploration in the ACK1 binding region.

Overall, we noticed 2-chloro-6-fluorocarboxamide as the R^1 group significantly contributed to the ACK1 inhibitory activities in compounds **9n**, **9m**, **20**, **9o**, and **22** (entries 13, 16, 19, 23, and 27, Table 1). **9o** (entry 23, Table 1) with 2-chloro-6-fluorocarboxamide as R^1 and *p*-(4-piperidinyl)aniline as R^3 showed markedly improved ACK1 inhibition with an IC_{50} of 53.3 nM, which is 3–4-fold more potent compared to the related **9f** with an IC_{50} of 231 nM and **9k** with an IC_{50} of 169 nM (entries 21 and 22, Table 1), which have Cl and Br, respectively. Similarly, compound **9s** (entry 26, Table 1) with piperidinecarboxylic acid as R^3 and 2-chloro-6-fluorocarboxamide as R^1 showed significantly improved ACK1 inhibition with an IC_{50} of 34 nM in the enzymatic assay compared to its related Cl and Br analogues **9e** (IC_{50} of 85 nM) and **9j** (85% inhibition at 10 μM), respectively (entries 24 and 25, Table 1). The improved inhibitory activities of **9n**, **9m**, **20**, **9o**, and **9s** (entries 13, 16, 19, 23, and 26, Table 1) can be attributed to the 2-chloro-6-fluorocarboxamide group in the 5-position of the pyrimidine undergoing a key H-bond contact in the gatekeeper region (see Figure 4A). Altogether, our SAR demonstrates that Cl and Br groups are tolerated in the 5-position of the pyrimidine core, and substitution of the 5-position with hydrogen as in compound **21** (entry 20, Table 1) considerably lowered the in vitro ACK1 affnity (16% at 10 μM, ELISA).

Although compounds **9n**, **9m**, **20**, **9o**, **9s**, and **22** with a 2-chloro-6-fluorocarboxamide moiety showed higher potency for ACK1 in the enzymatic assay, these compounds did not display the expected cellular potency most probably due to lack of cell permeability. Selected compounds from the set (±)-**9a–t** were chosen to evaluate the effects of ACK1 inhibition in LAPC4 human prostate cancer cells with inhibition of cell growth as the readout. The piperazine-substituted chloropyrimidine (±)-**9b** (entry 17, Table 1) showed

promising ACK1 inhibitory activities in cellular assays. On the basis of the findings from cell culture data, we synthesized enantiomers of **9b** to understand the ACK1 inhibitory activities of individual stereoisomers. The difference in activities of the two enantiomers is small. The (*R*)-**9b** isomer (Scheme 3) has marginally better ACK1 inhibitory activity with an IC_{50} of 56 nM, while (*S*)-**9b** has an IC_{50} of 82 nM in the ^{33}P HotSpot assay. The syntheses of (*R*)-**9b** and (*S*)-**9b** are shown in Scheme 3, and other examples of enantiomerically pure compounds (Table 2) were also synthesized using the protocols in Scheme 3. Both (*R*)-**9b** and (*S*)-**9b** were able to inhibit ACK1 autophosphorylation in prostate cancer cells (Figure 3a) and inhibit cell growth (Figure 3b–d).

Cell Culture Data of Selected Pyrimidines 9

ACK1 is a tyrosine kinase that autophosphorylates at Tyr284, which is indicative of its kinase activation. To determine the inhibitory potential of the representative pyrimidines **9**, the prostate cancer derived cell line LAPC4 was either treated with EGF ligand alone or added to cells pretreated with the compounds, and equal amounts of cell lysates were subjected to immuno-blotting. EGF ligand causes rapid activation of EGF receptor, which in turn leads to activation of the ACK1 kinase (Figure 3a, lane 2, top panel). In contrast, treatment of LAPC4 cells with (*R*)-**9b** and (*S*)-**9b** resulted in almost complete loss of ACK1 activation. The control ACK1 inhibitors **5** and **1b** also exhibited significant reduction in ACK1 activation. Actin was used as a control, which indicates equal loading of cell lysates (Figure 3a, lower panel).

In addition to (*R*)-**9b** and (*S*)-**9b**, we have also assessed other examples of **9** (Scheme 1) for their potential to suppress ACK1 kinase activity using immunoblotting, as described above. The inhibition (%) of ACK1 kinase activity is shown in Table 2.

Effects of (*R*)-9b and (*S*)-9b in Human Cancer Cells

Three distinct human prostate cancer derived cell lines, LNCaP, LAPC4, and VCaP, were either DMSO treated or treated with 1, 2.5, 5, 7.5, and 10 μM concentrations of inhibitors AIM-100, (*R*)-**9b**, and (*S*)-**9b** for 72 h, and the number of viable cells was counted by trypan blue exclusion assay. Both (*R*)-**9b** and (*S*)-**9b** were significantly better (IC_{50} = 1.8 μM) than AIM-100 (IC_{50} = 7 μM) in their ability to inhibit cell growth in LNCaP cells (Figure 3b). However, in LAPC4 cells, all three inhibitors were comparable in their ability to suppress cell proliferation (Figure 3c). In contrast, highly metastatic CRPC-forming VCaP cells were observed to be highly sensitive to (*R*)-**9b** (IC_{50} = 2 μM), while AIM-100 and (*S*)-**9b** exhibited an IC_{50} of 4 μM (Figure 3d). Taken together, it appears that (*R*)-**9b** is a superior ACK1 inhibitor *in vivo* and most significantly exhibits an ability to suppress proliferation of androgen-independent or CRPC VCaP cells.

Molecular Modeling of (±)-9b

The [(tetrahydrofurfuryl)amino]pyrimidine (*R*)-**9b** was docked to the catalytic domain of ACK1 (using GOLD[35,36] and the ACK1 crystal structure from PDB 4EWH) (Figure 4) to determine a representative binding mode and to study the structural features responsible for its binding to ACK1. In this pose, hydrogen bonding is predicted between the pyrimidine N1 atom and the B-ring NH to the ACK1 Ala208 residue (Figure 4A), typical of an

aminopyrimidine type 1 kinase inhibitor.[37] The chlorine atom is pointing toward, but not actually occupying, the hydrophobic pocket (highlighted in green in Figure 4A). This pocket is presumably occupied by the phenyl group in those derivatives that have an amide group at the pyrimidine 5-position (e.g., **9m** or **9s**). The tetrahydrofuryl group in (*R*)-**9b** orients itself closer to the ribose binding pocket of ACK1 and under the P-loop.

SAR Overview and Further Analogue Design

For the compounds synthesized as ACK1 inhibitors, the R^2 group was kept constant, while the 5-positions of the pyrimidine (R^1) and aniline (R^3) groups were changed. The SAR changes are highlighted in Figure 5a. Since the cell culture data indicated that (*R*)-**9b** and (*S*)-**9b** are potent in human cancer cells, we included Cl as R^1 in subsequent analogue synthesis. Therefore, on the basis of the cell culture data, SARs obtained for pyrimidines **9**, and inhibitory activities of compounds that contain a carboxylic acid tether such as in **9e**, **9j**, **9s**, and **22** (entries 24–27, Table 1), the compounds shown in Figure 5b with Cl in the 5-position of the pyrimidine as R^1 were synthesized to explore further SARs. Compounds **23**, **24**, **26**, and **28** (Figure 5b and Supporting Information) with one- or two-carbon-tethered carboxylic acids showed moderate ACK1 inhibition. The bisamine group in compound **26** (Figure 5b) was introduced with the hope of facilitating cell permeability and solubility. Compound **29** (Figure 5b) with a piperazine amide-tethered carboxylic acid showed significant ACK1 inhibition similar to that of compounds **22** (entry 27, Table 1). The *in vitro* activities of compounds shown in Figure 5b demonstrate the importance of the piperazine moiety to retain potent ACK1 inhibitory activities. On the basis of the SARs obtained in this study, we will continue our medicinal/synthetic chemistry efforts to further improve this class of compounds as novel ACK1 inhibitors, and broader SAR explorations will be discussed in future publications.

In Vitro PK Properties and Profiling of (*R*)-9b

Our cell culture data showed both (*R*)-**9b** and (*S*)-**9b** can penetrate human cancer cell lines and inhibit cell growth in an ACK1-dependent manner (Figure 3). The *in vitro* human plasma stabilities of compounds (*R*)-**9b** and (*S*)-**9b** were evaluated using HPLC analysis in a time-course experiment for up to 24 h (see Figure 6 and the Experimental Section). Our data showed both (*R*)-**9b** and (*S*)-**9b** were stable in human plasma (Figure 6) for up to 24 h and displayed a long half-life ($t_{1/2}$ > 6 h). Procaine and procainamide were used as standards to generate the human plasma stability data of (*R*)-**9b** and (*S*)-**9b** using HPLC analysis (Figure 6).[38] The solubilities of (*R*)-**9b** and (*S*)-**9b** were determined as 1 and 0.9 mg/mL, respectively, in PBS with 10% DMSO (clear solution). The solubility of the mesylate salt of (*R*)-**9b** in PBS with 10% DMSO was determined as >5 mg/mL, further suggesting its suitability for in vivo animal experiments. The most potent compound in the cell experiments, the [(tetrahydrofurfuryl)amino]pyrimidine (*R*)-**9b**, was subjected to limited profiling against 34 kinases using the Reaction Biology ^{33}P HotSpot kinase profiling service (Table 3) to determine its selectivity for ACK1. At 1 μM (*R*)-**9b** ACK1 was the kinase most potently inhibited (99.8%). Of the other kinases inhibited by >80%, the most notable were the JAK family kinases JAK2 (98.6%) and Tyk2 (98.9%). Only six other kinases were inhibited by >80%; these were ABL1 (82.8%), ALK (86.0%), CHK1 (84.8%), FGFR1

(86.4%), LCK (87.7%), and ROS/ROS1 (84.2%). Dose responses were obtained for these kinases inhibited by >80% at 1 μM: JAK2 (IC_{50} = 6 nM), Tyk2 (IC_{50} = 5 nM), FGFR1 (IC_{50} = 160 nM), ABL1 (IC_{50} = 206 nM), CHK1 (IC_{50} = 154 nM), ALK (IC_{50} = 143 nM), LCK (IC_{50} = 136 nM), and ROS/ROS1 (IC_{50} = 124 nM). Interestingly we have seen that other diaminopyrimidines also give rise to potent JAK inhibition.[32,33,39] To assess JAK2 activation in prostate cancer epithelial cells, LNCaP and LAPC4 were treated with heregulin or EGF ligands, respectively, followed by immunoblotting with phospho-ACK1 (Tyr284), phospho-JAK2 (Tyr1007), and phospho-STAT5 (Tyr694) antibodies. While significant ACK1 activation was observed in EGF-treated LAPC4 and LNCaP prostate cancer epithelial cells, neither JAK2 nor STAT5 activation was observed (unpublished data), suggesting that ACK1 and JAK2 kinase activations are distinct events that occur in different cellular contexts. Since several ALK inhibitors[26,40] also inhibit ACK1 and (*R*)-**9b** was partly designed from an ALK inhibitor, its IC_{50} for ALK inhibition was measured using the HotSpot assay and found to be 143 nM, 3-fold less than the IC_{50} for ACK1. The superposition of the pose of (*R*)-**9b** in ACK1 with crystal structures of both ALK and JAK2 shows a reasonable fit in each case (see the Supporting Information, Figures S1 and S2). It is also known that Src kinase is a regulator of the androgen receptor.[40] The IC_{50} for (*R*)-**9b** against cSrc was 438 nM, 10-fold less than the IC_{50} for ACK1. Overall, the selectivity of (*R*)-**9b** for ACK1 and JAK2 appears to be good.

CONCLUSION

A combination of a fragment-based approach of creating small-molecule libraries using a bisanilinopyrimidine scaffold and a novel ELISA-based assay of screening the compound libraries for their inhibitory potential led to the identification of a novel class of ACK1 inhibitors. The SARs showed tetrahydrofurfurylamine as R^2 and a piperazine moiety as R^3 are critical for ACK1 inhibitory activities with (*R*)-**9b** and (*S*)-**9b** discovered as potent compounds using ELISA and ^{33}P HotSpot assays. Compounds (*R*)-**9b** and (*S*)-**9b** were also shown to be potent ACK1 inhibitors in vivo, suppressing the growth of the prostate cancer derived cell lines. Furthermore, (*R*)-**9b** and (*S*)-**9b** displayed selectivity toward ACK1 when compared with other related tyrosine kinases such as Src and ALK, but potently inhibited the JAK family kinases JAK2 and Tyk2. The binding mode of compound **9b** described here provides further opportunities to improve this class of compounds as ACK1 inhibitors. Overall, the availability of potent and selective ACK1 inhibitors has opened the doors for preclinical animal studies that could lead to clinical trials for hormonally regulated cancers such as prostate and breast cancers.

EXPERIMENTAL SECTION

Assessment of ACK1 Inhibition via ELISA

In brief, biotinylated AKT peptide (5 μM) was immobilized onto a streptavidin-coated 96-well plate, followed by blocking with 3% BSA. ACK1 enzyme purified from SF9 cells (40 ng/reaction) was resuspended in a reaction buffer (10 mM HEPES, 20 mM $MgCl_2$, 75 mM NaCl, and 1 mM DTT) and added to the plate in the presence of the compounds (10 μM). After incubation for 1 h at 37 °C, the plates were washed, blocked, and incubated with HRP-

tagged anti-pTyr antibodies (1:500) for 1 h. Alternately, anti-pY176-AKT phosphoantibodies (1:100) were used, followed by secondary anti-rabbit antibodies. The plates were developed using SigmaFast OPD substrate solution (Sigma, St. Louis, MO) and read with a spectrophotometer.

General Chemistry Information

All reagents were purchased from commercial suppliers and used without further purification. ^{1}H NMR spectra were recorded on an Agilent-Varian Mercury 400 MHz spectrometer with $CDCl_3$, CD_3OD, or DMSO-d_6 as the solvent. ^{13}C NMR spectra were recorded at 100 MHz. All coupling constants are measured in hertz, and the chemical shifts (δ_H and δ_C) are quoted in parts per million relative to TMS (δ 0), which was used as the internal standard. High-resolution mass spectroscopy was carried out on an Agilent 6210 LC–MS (ESI-TOF) system. Microwave reactions were performed in CEM model 908005 and Biotage Initiator 8 machines. HPLC analysis was performed using a JASCO HPLC system equipped with a PU-2089 Plus quaternary gradient pump and a UV-2075 Plus UV–vis detector, using an Alltech Kromasil C-18 column (150 × 4.6 mm, 5 μm) and an Agilent Eclipse XDB-C18 column (150 × 4.6 mm, 5 μm). The purities of the final compounds that underwent biological assessment were >95% as measured by HPLC. Melting points were recorded on an Optimelt automated melting point system (Stanford Research Systems). Thin-layer chromatography was performed using silica gel 60 F254 plates (Fisher), with observation under UV when necessary. Anhydrous solvents (acetonitrile, dimethylformamide, ethanol, 2-propanol, methanol, and tetrahydrofuran) were used as purchased from Aldrich. Burdick and Jackson HPLC-grade solvents (methanol, acetonitrile, and water) were purchased from VWR for HPLC and high-resolution mass analysis. HPLC-grade TFA was purchased from Fisher.

2,4-Dichloropyrimidine-5-carbonyl Chloride (Scheme 2)

To $POCl_3$ (45 mL, 0.071 mol) in a round-bottom flask was added 2,4-dihydroxypyrimidine-5-carboxylic acid (10.00 g, 0.064 mol) portionwise at 0 °C, followed by slow addition of PCl_5 (46.60 g, 0.229 mol). The reaction mixture was warmed to rt and heated to reflux for 16 h. The mixture was concentrated to dryness and slurried with DCM (30 mL), and the solid precipitated was filtered and washed with DCM (2 × 20 mL). The filtrate was evaporated under reduced pressure to afford the title compound (13.90 g, 99%) as a yellow oil. ^{1}H NMR (400 MHz, $CDCl_3$): δ 9.25 (s, 1H).[31]

2,4-Dichloro-*N*-(2-chloro-6-fluorophenyl)pyrimidine-5-carboxamide (7c)

To a solution of 2,4-dichloropyrimidine-5-carbonyl chloride (6.36 g, 0.030 mol) (obtained in the previous step) in THF (40 mL) under inert conditions was added 2-chloro-6-fluoroaniline (4.38 g, 0.03 mol) portionwise, and the reaction mixture was stirred at rt for 15 h. The resulting precipitate was filtered and washed with DCM (15 mL), and the solid obtained was sonicated in HCl (1 M, 100 mL), filtered, washed with water (20 mL) and DCM (20 mL) sequentially, and dried under high vacuum to obtain the title compound **7c** (5.53 g) as a white solid. The first filtrate (i.e., THF and DCM mixture) was concentrated, slurried with DCM (15 mL), and filtered to get a second crop of solid. This solid was again

sonicated with HCl (1 M, 30 mL), filtered, washed with water (20 mL) and DCM (15 mL) sequentially, and dried under high vacuum to obtain another crop of pure product **7c** (1.70 g) also as a white solid. The combined yield of **7c** was 7.23 g (75%). Mp: 207–211 °C. ^{1}H NMR (400 MHz, DMSO-d_6): δ 10.71 (s, 1H), 9.03 (s, 1H), 7.48–7.36 (m, 3H). ^{19}F NMR (376 MHz, DMSO-d_6): –115.25 to –115.28 (m). LC–MS (ESI+): *m/z* 319.96 $(M + H)^+$. HRMS (ESI+): *m/z* calcd for $C_{11}H_6Cl_3FN_3O$ $(M + H)^+$ 319.9555, found 319.9562.

2,5-Dichloro-*N*-[(tetrahydrofuran-2-yl)methyl]pyrimidin-4-amine [(±)-8a]

Tetrahydrofurfurylamine (1.251 g, 12.36 mmol) in MeOH (11 mL) was added dropwise to a solution of 2,4,5-trichloropyrimidine (2.27 g, 12.36 mmol) and triethylamine (1.251 g, 12.36 mmol) in MeOH (11 mL) at 0 °C and stirred for 1.5 h under argon. The reaction mixture was warmed to room temperature, and the solvent was removed under reduced pressure. The residue obtained was dissolved in DCM. The organic layer was washed with water, dried, and concentrated to afford **8a** as a yellow solid (2.86 g, 93%). Mp: 81–84 °C. HPLC: 92.0% [t_R = 11.17 min, 30% CH_3OH in 0.1% TFA/water, 20 min]. ^{1}H NMR (400 MHz, methanol-d_4) δ 8.01 (s, 1H), 4.16–4.09 (m, 1H), 3.91–3.85 (m, 1H), 3.78–3.72 (m, 1H), 3.60–3.48 (m, 2H), 2.06–1.83 (m, 3H), 1.70–1.58 (m, 1H). LC–MS (ESI+): *m/z* 248.03536 $(M + H)^+$. HRMS (ESI+): *m/z* calcd for $C_9H_{11}Cl_2N_3O^+$ $(M + H)^+$ 248.0352, found 248.0359.

5-Bromo-2-chloro-*N*-[(tetrahydrofuran-2-yl)methyl]-pyrimidin-4-amine [(±)-8b]

This compound was synthesized using the same procedure described for **8d** except using 5-bromo-2,4-dichloropyrimidine (0.500 g, 2.195 mmol) in MeOH (2 mL) and tetrahydrofurfurylamine (0.222 g, 2.195 mmol) in MeOH (2 mL) and triethylamine (0.305 mL, 2.195 mmol) to afford **8b** as a white solid (0.620 g, 97%). Mp: 85–86 °C. ^{1}H NMR (400 MHz, DMSO-d_6): δ 8.23 (s, 1H), 7.62 (br s, 1H), 4.03–3.98 (m, 1H), 3.77–3.71 (m, 1H), 3.62–3.57 (m, 1H), 3.45–3.38 (m, 1H), 3.36–3.30 (m, 1H), 1.90–1.75 (m, 3H), 1.60–1.52 (m, 1H). HPLC–MS (ESI+): *m/z* 292 and 294.1 for Br isotopes $(M + H)^+$.

2-Chloro-*N*-(2-chloro-6-fluorophenyl)-4-[[(tetrahydrofuran-2-yl)methyl]amino]pyrimidine-5-carboxamide [(±)-8c]

To a solution of tetrahydrofurfurylamine (0.121 g, 1.2 mmol) in MeOH (2 mL) was added triethylamine (0.167 mL, 1.2 mmol) at 0 °C under an inert atmosphere. After the resulting solution was stirred at 0 °C for 10 min, **7c** (0.320 g, 1.0 mmol) in DMF (0.5 mL) was added dropwise. The mixture was warmed to rt and stirred for 30 min. The solvent was removed, and the crude mixture was purified by SiO_2 chromatography (0–30% gradient elution, EtOAc/hexane) to afford **8c** as a pure white solid (0.283 g, 74%). Mp: 142 °C dec. ^{1}H NMR (400 MHz, $CDCl_3$): δ 8.88 (br t, 1H), 8.55 (s, 1H), 7.58 (br s, 1H), 7.30–7.23 (m, 2H), 7.15–7.12 (m, 1H), 4.12–4.06 (m, 1H), 3.91–3.85 (m, 1H), 3.80–3.72 (m, 2H), 3.54–3.48 (m, 1H), 2.07–1.99 (m, 1H), 1.94–1.86 (m, 2H), 1.64–1.56 (m, 1H). LC–MS (ESI+): *m/z* 385.07 $(M + H)^+$. HRMS (ESI+): *m/z* calcd for $C_{16}H_{16}Cl_2FN_4O_2$ $(M + H)^+$ 385.0629, found 385.0623.

2-Chloro-5-fluoro-*N*-[(tetrahydrofuran-2-yl)methyl]pyrimidin-4-amine [(±)-8d]

To a solution of tetrahydrofurfurylamine (0.607 g, 6 mmol) in MeOH (10 mL) was added triethylamine (836 μL) under argon at 0 °C. The mixture was stirred at 0 °C for 10 min, and

then 2,4-dichloro-5-fluoropyrimidine (0.835 g, 5 mmol) in MeOH (4 mL) was added dropwise at 0 °C. The reaction mixture was warmed to room temperature and stirred for 2 h. The solvent was removed, and the resulting precipitate was dissolved in EtOAc (30 mL) and washed with water (2 × 20 mL). The organic phase was dried (Na_2SO_4), filtered, and concentrated. The crude material obtained was purified by SiO_2 chromatography (silica gel, 20 g, EtOAc/hexane, 0–25%) to afford **8d** as a white solid (0.936 g, 81%). Mp: 77–78 °C. ^{1}H NMR (400 MHz, $CDCl_3$): δ 7.86 (d, J = 2.8 Hz, 1 H), 5.63 (br s, 1H), 4.08 (ddd, J = 14.8, 7.2, 3.2 Hz, 1 H), 3.92–3.76 (m, 3H), 3.37 (ddd, J = 13.6, 8.0, 4.4 Hz, 1 H), 2.10–2.02 (m, 1 H), 1.97–1.90 (m, 2H), 1.64–1.56 (m, 1H). HPLC–MS (ESI+): *m/z* 232.1 $(M + H)^+$.

2-Chloro-5-methyl-*N*-[(tetrahydrofuran-2-yl)methyl]pyrimidin-4-amine [(±)-8e]

This compound was synthesized according to the procedure described for **8d** except using 2,4-dichloro-5-methylpyrimidine (2.680 g, 16.440 mmol) in MeOH (20 mL) and tetrahydrofurfurylamine (1.997 g, 19.730 mmol) in MeOH (5 mL) and triethylamine (2.750 mL) to afford **8e** as a white solid (1.997 g, 53%). Mp: 86–89 °C. ^{1}H NMR (400 MHz, $CDCl_3$): δ 7.78 (d, J = 0.8 Hz, 1H), 5.24 (br s, 1H), 4.08–4.04 (m, 1H), 3.90–3.81 (m, 2H), 3.80–3.74 (m, 1H), 3.33 (ddd, J = 13.6, 8.0, 4.4 Hz, 1H), 2.08–2.01 (m, 1H), 1.99 (app d, J = 0.8 Hz, 3H), 1.95–1.88 (m, 2H), 1.63–1.54 (m, 1H). HPLC–MS (ESI+): *m/z* 228.1 $(M + H)^+$.

(*R*)-2,5-Dichloro-*N*-[(tetrahydrofuran-2-yl)methyl]pyrimidin-4-amine [(*R*)-8f]

(*R*)-(–)-Tetrahydrofurfurylamine (0.992 g, 9.81 mmol) in MeOH (10 mL) was added to a solution of 2,4,5-trichloropyrimidine (1.00 g, 5.45 mmol) in MeOH (10 mL) and triethylamine (9.81 mmol) at 0 °C for 1 h under argon. The solution was then warmed to room temperature and stirred for 2 h. The solvent was removed under reduced pressure, and the solid obtained was suspended in chloroform and washed with $NaHCO_3$(aq). The organic layer was separated, dried (Na_2SO_4), concentrated, and further dried under vacuum to afford (*R*)-**8f**) as a white solid (1.354 g, 87%). Mp: 61.5–61.8 °C. HPLC: 97.3% [t_R = 3.36 min, 70% CH_3OH in 0.1% TFA/water, 20 min]. ^{1}H NMR (400 MHz, $CDCl_3$) δ 8.01 (s, 1H), 5.91 (s, 1H), 4.12–4.06 (m, 1H), 3.91–3.88 (m, 1H), 3.85–3.77 (m, 2H), 3.44–3.37 (m, 1H), 2.09–2.01 (m, 1H), 1.97–1.90 (m, 2H), 1.60–1.57 (m, 1H). LC–MS (ESI+): *m/z* 247.02792 $(M + H)^+$. HRMS (ESI+): *m/z* calcd for $C_9H_{11}C_{l2}N_3O^+$ $(M + H)^+$ 248.0352, found 248.0368.

(*S*)-2,5-Dichloro-*N*-[(tetrahydrofuran-2-yl)methyl]pyrimidin-4-amine [(*S*)-8f]

To a solution of (*S*)-(–)-tetrahydrofurfurylamine (0.992 g, 9.81 mmol) in MeOH (10 mL) was added triethylamine (1.3 mL, 9.81 mmol) at 0 °C. The solution was stirred for 10 min and added to a solution of 2,4,5-trichloropyrimidine (1.00 g, 5.45 mmol) in MeoH (4 mL) dropwise also at 0 °C. The solution was then warmed to room temperature and stirred for 2 h. The solvent was removed under reduced pressure, and the solid was dissolved in chloroform, washed with satd $NaHCO_3$(aq). The organic layer was separated, dried (Na_2SO_4), filtered, and concentrated to afford the chloropyrimidine (*S*)-**8f** as a white solid (1.054 g, 68%). Mp: 59.2–60.0 °C. HPLC: 95.4% [t_R = 3.36 min, 70% CH_3OH in 0.1% TFA/water, 20 min]. ^{1}H NMR (400 MHz, $CDCl_3$) δ 8.01 (s, 1H), 5.91 (br s, 1H), 4.09 (ddd, J = 7.2, 4.2, 3.2 Hz, 1H), 3.94–3.88 (m, 1H), 3.85–3.77 (m, 2H), 3.44–3.37 (m, 1H), 2.09–

2.01 (m, 1H), 1.97–1.89 (m, 2H), 1.62–1.54 (m, 1H). LC–MS (ESI+): *m/z* 247.02792 (M + H)$^+$. HRMS (ESI+): *m/z* calcd for $C_9H_{11}C_{l2}N_3O^+$ (M + H)$^+$ 248.0352, found 248.0353.

5-Chloro-*N*^{2}-[4-(piperazin-1-yl)phenyl]-*N*^{4}-[(tetrahydrofuran-2-yl)methyl]pyrimidine-2,4-diamine [(±)-9a]

The chloropyrimidine **8a** (0.100 g, 0.403 mmol) and 1-Boc-4-(4′-aminophenyl)-piperazine (0.112 g, 0.403 mmol) were mixed in EtOH (1 mL) in a 5 mL microwave vial and heated to 150 °C for 20 min in a microwave reactor, after which a drop of concentrated HCl was added before the solution was returned to the microwave for a further 20 min at 150 °C. The precipitate formed was filtered and washed with saturated $NaHCO_3$. The white solid was dried under reduced pressure to obtain **9a** (0.074 g, 0.190 mmol, 47%). HPLC: 97.8% [t_R = 6.99 min, gradient MeOH/water, 5–95% (with 0.1% formic acid), 20 min]. ^{1}H NMR (400 MHz, DMSO-d_6) δ 8.93 (s, 1H), 7.86 (s, 1H), 7.50 (d, *J* = 9.0 Hz, 2H), 7.00 (t, *J* = 5.7 Hz, 1H), 6.79 (d, *J* = 9.1 Hz, 2H), 4.10–4.03 (m, 1H), 3.75 (dd, *J* = 13.6, 7.5 Hz, 1H), 3.60 (dd, *J* = 14.5, 7.4 Hz, 1H), 3.41 (t, *J* = 6.0 Hz, 3H), 2.91 (t, *J* = 4.0 Hz, 4H), 2.79 (t, *J* = 4.8 Hz, 4H), 1.92–1.77 (m, 3H), 1.62–1.56 (m, 1H). HPLC–MS (ESI): *m/z* 195.2 [(M + 2H)/2]$^{2+}$. LC–MS (ESI+): *m/z* 389.19 (M + H)$^+$. HRMS (ESI+): *m/z* calcd for $C_{19}H_{26}ClN_6O^+$ (M + H)$^+$ 389.1851, found 389.1860.

5-Chloro-*N*^{2}-[4-(4-methylpiperazin-1-yl)phenyl]-*N*^{4}-[(tetrahydrofuran-2-yl)methyl]pyrimidine-2,4-diamine [(±)-9b]

The chloropyrimidine **8a** (0.200 g, 0.806 mmol) and 4-(4-methylpiperazin-1-yl)aniline (0.170 g, 0.889 mmol) were mixed in a microwave vial with HCl (200 μL of 4 M solution in dioxane). 2-Methoxyethanol (6.50 mL) was added, the vial was sealed, and the solution was heated to 110 °C for 48 h. The resulting solution was concentrated under reduced pressure, and the product was partitioned between $CHCl_3$ and saturated aqueous $NaHCO_3$. The organic phase was then dried over Na_2SO_4, filtered, and concentrated under reduced pressure. The resulting product was purified (silica gel, 5:95 methanol/dichloromethane) to afford (±)-**9b** as a pure white solid (0.108 g, 33%). Mp: 133 °C dec. HPLC: 95.3% [t_R = 7.10 min, gradient MeOH/water, 5–95% (with 0.1% formic acid), 20 min]. ^{1}H NMR (400 MHz, CD_3OD) δ 7.77 (s, 1H), 7.46 (d, *J* = 8.8 Hz, 2H), 6.93 (d, *J* = 8.8 Hz, 2H), 4.20–4.14 (m, 1H), 3.88–3.83 (m, 1H), 3.78–3.70 (m, 1H), 3.58 (dd, *J* = 13.6, 4.8 Hz, 1H), 3.48 (dd, *J* = 13.6, 4.8 Hz, 1H), 3.14 (t, *J* = 4.8 Hz, 4H), 2.62 (t, *J* = 5.2 Hz, 4H), 2.38 (s, 3H), 2.04–1.80 (m, 3H), 1.70–1.59 (m, 1H). HPLC–MS (ESI): *m/z* 202.3 [(M + 2H)/2]$^{2+}$. LC–MS (ESI+): *m/z* 403.20 (M + H)$^+$. HRMS (ESI+): *m/z* calcd for $C_{20}H_{28}ClN_6O^+$ (M + H)$^+$ 403.2007, found 403.2008.

Development of Analytical Chiral HPLC Conditions for Separation of (±)-9b

Analytical HPLC was performed using a JASCO HPLC system equipped with a PU-2089 Plus quaternary gradient pump and a UV-2075 Plus UV–vis detector using a Chiralcel OJ column (250 × 4.6 mm). The racemic mixture (±)-**9b** was separated with 15% IPA and 85% hexane, 1.0 mL/min, and chromatography yielded a faster eluting peak, t_R = 57.7 min (*R*-isomer), and a slower eluting peak, t_R = 83.5 min (*S*-isomer).

(*R*)-5-Chloro-*N*^{2}-[4-(4-methylpiperazin-1-yl)phenyl]-*N*^{4}-[(tetrahydrofuran-2-yl)methyl]pyrimidine-2,4-diamine [(*R*)-9b]

The chloropyrimidine (*R*)-**8f** (0.200 g, 0.806 mmol) and 4-(4-methylpiperazin-1-yl)aniline (0.170 g, 0.889 mmol) were mixed in a microwave tube with HCl (200 μL of 4 M solution in dioxane). 2-Methoxyethanol (6.50 mL) was added to the mixture, and the solution was warmed to 110 °C for 48 h. The reaction mixture was concentrated, and the product was partitioned between $CHCl_3$ and saturated aqueous $NaHCO_3$. The organic phase was then dried over Na_2SO_4, filtered, and concentrated. The product was purified using a silica gel column with 5:95 methanol/dichloromethane to afford the pure compound (*R*)-**9b** as a white solid (0.220 g, 68%). Mp: 135 °C dec. $[\alpha]_D$ –12 (*c* 0.25 in MeOH). HPLC: 96% [t_R = 6.11 min, 30% CH_3OH in 0.1% TFA/water, 20 min]. ^{1}H NMR (400 MHz, CD_3OD) δ 7.82 (s, 1H), 7.50 (d, *J* = 8.8 Hz, 2H), 6.97 (d, *J* = 8.8 Hz, 2H), 4.22–4.16 (m, 1H), 3.94–3.88 (m, 1H), 3.81–3.76 (m, 1H), 3.63 (dd, *J* = 13.6, 4.8 Hz, 1H), 3.53 (dd, 13.6, 4.8 Hz, 1H), 3.18 (t, *J* = 4.8 Hz, 4H), 2.67 (t, *J* = 5.2 Hz, 4H), 2.34 (s, 3H), 2.03–1.86 (m, 3H), 1.70–1.63 (m, 1H). ^{13}C NMR (100 MHz, methanol-d_4): δ 158.38, 158.08, 152.19, 146.49, 133.46, 120.97, 116.74, 103.51, 77.46, 67.61, 54.59, 49.48, 44.66, 44.18, 28.43, 25.15. LC–MS (ESI+): *m/z* 403.2007 $(M + H)^+$. HRMS (ESI+): *m/z* calcd for $C_{20}H_{27}ClN_6O^+$ $(M + H)^+$ 403.2008, found 403.2004. Chiral HPLC: 96% [t_R = 43.18 min, 15% IPA and 85% hexane, 1.0 mL/min].

(*S*)-5-Chloro-*N*^{2}-[4-(4-methylpiperazin-1-yl)phenyl]-*N*^{4}-[(tetrahydrofuran-2-yl)methyl]pyrimidine-2,4-diamine [(*S*)-9b]

The chloropyrimidine (*S*)-**8f** (0.372 g, 1.5 mmol) and 4-(4-methylpiperazin-1-yl)aniline (0.316 g, 1.65 mmol) were mixed in a microwave vial with HCl (0.412 mL of a 4 M solution in dioxane). The 2-methoxyethanol (8.0 mL) was added to the mixture, the vial was sealed, and the solution was heated to 110 °C for 48 h. The resulting solution was concentrated under reduced pressure, and the product was partitioned between $CHCl_3$ and saturated aqueous $NaHCO_3$. The organic phase was separated, then dried over Na_2SO_4, filtered, and concentrated under reduced pressure. The product obtained was purified using a silica gel column with 5:95 methanol/dichloromethane to afford the pure compound (*S*)-**9b** as a white solid (475 mg, 79%). Mp: 145 °C dec. $[\alpha]_D$ +9.6 (*c* 0.25 in MeOH). HPLC: 98% [t_R = 6.85 min, 30% CH_3OH in 0.1% TFA/water, 20 min]. ^{1}H NMR (400 MHz, CD_3OD) δ 7.77 (s, 1H), 7.45 (d, *J* = 8.8 Hz, 2H), 6.94 (d, *J* = 8.8 Hz, 2H), 4.17–4.14 (m, 1H), 3.89–3.84 (m, 1H), 3.77–3.71 (m, 1H), 3.63 (dd, *J* = 13.6, 4.8 Hz, 1H), 3.50 (dd, 13.6, 4.8 Hz, 1H), 3.14 (t, *J* = 4.8 Hz, 4H), 2.62 (t, *J* = 4.8 Hz, 4H), 2.34 (s, 3H), 2.02–1.88 (m, 3H), 1.70–1.63 (m, 1H). LC–MS (ESI+): *m/z* 403.20076 $(M + H)^+$. HRMS (ESI+): *m/z* calcd for $C_{20}H_{27}ClN_6O^+$ $(M + H)^+$ 403.19349, found 403.20079. Chiral HPLC: 100% [t_R = 32.4 min, 15% IPA and 85% hexane, 1.0 mL/min].

5-Chloro-*N*^{2}-(4-morpholinophenyl)-*N*^{4}-[(tetrahydrofuran-2-yl)methyl]pyrimidine-2,4-diamine Hydrochloride [(±)-9c]

The chloropyrimidine **8a** (0.100 g, 0.403 mmol) and 4-morpholinoaniline (0.072 g, 0.403 mmol) were mixed in EtOH (3 mL) in a 5 mL microwave vial and heated to 150 °C for 20 min in a microwave reactor. The solid obtained upon cooling was filtered, washed with ethyl acetate, and dried under vacuum to afford **9c** as an off-white solid (0.072 g, 0.185 mmol,

46%). Mp: 221.4 °C dec. HPLC: 99.0% [t_R = 9.90 min, gradient MeOH/water, 5–95% (with 0.1% formic acid), 20 min]. ^{1}H NMR (400 MHz, CD_3Cl3) δ 10.32 (s, 1H), 7.67 (s, 1H), 7.45 (dd, *J* = 8.8 Hz, 2H), 6.90 (d, *J* = 8.4 Hz, 2H), 6.62 (app t, *J* = 5.6 Hz, 1H), 4.13–4.06 (m, 1H), 3.92–3.86 (m, 5H), 3.82–3.77 (m, 1H), 3.46–3.40 (m, 1H), 3.15 (t, *J* = 4.8 Hz, 4H), 2.08–2.00 (m, 1H), 1.981.91 (m, 2H), 1.61–1.52 (m, 1H). LC–MS (ESI+): *m/z* 390.17 (M-Cl)$^+$. HRMS (ESI+): *m/z* calcd for $C_{19}H_{25}ClN_5O_2^+$ (M – Cl)$^+$ 390.1691, found 390.1694.

5-Chloro-*N*^{2}-[4-(piperidin-1-ylmethyl)phenyl]-*N*^{4}-[(tetrahydrofuran-2-yl)methyl]pyrimidine-2,4-diamine [(±)-9d]

The chloropyrimidine **8a** (0.100 g, 0.403 mmol) and 4-(piperidinylmethyl)aniline (0.107 g, 0.564 mmol) were mixed in 2-methoxyethanol (1.5 mL), and HCl (0.05 mL of a 12 M aq solution) was added. The reaction mixture was heated in an oil bath at 120 °C with stirring for 5.5 h and then allowed to cool to room temperature. The solvent was evaporated, and saturated $NaHCO_3$ (10 mL) was added, followed by EtOAc (20 mL). The organic layer was extracted with water, dried ($MgSO_4$), and evaporated. The resulting solid was slurried in diethyl ether and filtered to afford the required product **9d** as a white powder (0.051 g, 31%). Mp: 120.3–121.7 °C. HPLC: 98.0% [t_R = 8.09 min, gradient MeOH/water, 5–95% (with 0.1% formic acid), 20 min]. ^{1}H NMR (400 MHz, CD_3OD) δ 7.82 (s, 1H), 7.57 (d, *J* = 8.6 Hz, 2H), 7.22 (d, *J* = 8.6 Hz, 2H), 4.22–4.13 (m, 1H), 3.89 (dd, *J* = 13.3, 6.6 Hz, 1H), 3.75 (dd, *J* = 14.3, 7.4 Hz, 1H), 3.58 (dd, *J* = 13.6, 4.8 Hz, 1H), 3.52 (dd, *J* = 14.0, 6.8 Hz, 1H), 3.45 (s, 2H), 2.43 (br s, 4H), 2.08–1.83 (m, 3H), 1.73–1.64 (m, 1H), 1.64–1.55 (m, 4H), 1.46 (br s, 2H). LC–MS (ESI+): *m/z* 317.12 (M – piperidine)$^+$. HPLC–MS: *m/z* 201.7 [(M + 2H)/2]$^{2+}$. HRMS (ESI+): *m/z* calcd for $C_{21}H_{29}ClN_5O^+$ (M + H)$^+$ 402.2055, found 402.2063.

5-Chloro-*N*^{2}-{4-[4-(carboxyethyl)piperidinyl]phenyl}-*N*^{4}-[(tetrahydrofuran-2-yl)methyl]pyrimidine-2,4-diamine Hydrochloride [Intermediate for (±)-9e]

A suspension of **8a** (0.100 g, 0.403 mmol) and ethyl 1-(4-aminophenyl)piperidine-4-carboxylate (0.200 g, 0.806 mmol) in EtOH (4 mL) was heated in a microwave reactor at 150 °C for 20 min. The resulting mixture was concentrated, and the residue obtained was recrystallized with EtOAc/hexane (5 mL, 1:2). The mixture was filtered and the solid dried under high vacuum to afford the title compound **9e** as a gray solid (0.273 g, 68%). Mp: 113 °C dec. HPLC: 99.0% [t_R = 5.65 min, 45% CH_3OH in 0.1% TFA/water, 20 min]. ^{1}H NMR (400 MHz, CD_3OD): δ 7.88 (s, 1H), 7.49 (br s, 2H), 7.26 (br s, 2H), 4.19–4.14 (m, 3H), 3.88–3.82 (m, 1H), 3.77–3.68 (m, 3H), 3.58 (d, *J* = 5.6 Hz, 2H), 3.21–3.12 (m, 2H), 2.61 (app t, 1H), 2.10 (app d, 2H), 2.03–1.85 (m, 5H), 1.69–1.60 (m, 1H), 1.27 (t, *J* = 6.8 Hz, 3H). LC–MS (ESI+): *m/z* 460.2 (M + H)$^+$. HRMS (ESI+): *m/z* calcd for $C_{23}H_{31}ClN_5O_3$ (M + H)$^+$ 460.2110, found 460.2112.

5-Chloro-*N*^{2}-[4-(4-carboxypiperidinyl)phenyl]-*N*^{4}-[(tetrahydrofuran-2-yl)methyl]pyrimidine-2,4-diamine [(±)-9e]

To a suspension of the compound prepared in the above step (0.272 g, 0.548 mmol) in THF (2.192 mL) was added NaOH (2 M, 1.096 mL). The reaction mixture was stirred at room temperature for 18 h. The THF was removed, water was added (2 mL), and extraction with DCM (2 mL) was performed. The aqueous solution was acidified with HCl (1 M) to pH 4–5.

The resulting precipitate was filtered and washed with water (5 mL × 4), then quickly washed with MeOH (2 mL), and dried under high vacuum to afford the first crop of the required compound (0.112 g). The solid precipitated in the filtrate was filtered, washed with water (5 mL × 2), and dried under high vacuum to afford the second crop of the required compound (0.096 g). The solids were combined to afford **9e** as a pure dark gray solid (0.208 g, 81%). Mp: 93 °C dec. HPLC: 99.0% [t_R = 8.59 min, 30% CH_3OH in 0.1% TFA/water, 20 min]. ^{1}H NMR (400 MHz, CD_3OD): δ 7.81 (s, 1H), 7.46 (d, J = 8.4 Hz, 2H), 7.09 (d, J = 8.8 Hz, 2H), 4.20–4.13 (m, 1H), 3.89–3.84 (m, 1H), 3.77–3.72 (m, 1H), 3.62–3.48 (m, 4H), 2.79 (dt, J = 11.2, 2.4 Hz, 2H), 2.45 (tt, J = 11.2, 4.0 Hz, 1H), 2.06–1.80 (m, 7H), 1.70–1.62 (m, 1H). LC–MS (ESI+): *m/z* 432.17; $(M + H)^+$. HRMS (ESI+): *m/z* calcd for $C_{21}H_{27}ClN_5O_3$ $(M + H)^+$ 432.1796, found 432.1796.

4-(Piperidin-4-yl)aniline [Intermediate for (±)-9f]

To a solution of 4-(4-nitrophenyl)piperidine (400 mg, 1.942 mmol) in MeOH (30 mL) was added Pd on carbon (144 mg) under argon. The argon was removed, and H_2 gas was introduced into the system. After 3.5 h at room temperature, the palladium catalyst was filtered, and the solvent was removed. The residue was purified by trituration with DCM to afford 4-(piperidin-4-yl)aniline as a white solid (340 mg, 99%). Mp: 162.7 °C. HPLC: 95.0% [t_R = 6.74 min, 30% CH_3OH in 0.1% TFA/water, 20 min]. ^{1}H NMR (400 MHz, methanol-d_4) δ 6.99 (d, J = 8.4 Hz, 2H), 6.69 (d, J = 8.4 Hz, 2H), 3.46–3.22 (m, 2H), 2.95 (td, J = 12.8, 3.0 Hz, 2H), 2.70–2.62 (m, 1H), 1.96–1.84 (m, 2H), 1.82–1.70 (m, 2H). LC–MS (ESI+): *m/z* 177.13808 $(M + H)^+$. HRMS (ESI+): *m/z* calcd for $C_{11}H_{16}N_2^+$ $(M + H)^+$ 177.1386, found 177.1382.

5-Chloro-*N*^{2}-[4-(piperidin-4-yl)phenyl]-*N*^{4}-[(tetrahydrofuran-2-yl)methyl]pyrimidine-2,4-diamine [(±)-9f]

The chloropyrimidine **8a** (80 mg, 0.32 mmol) and 4-(piperidin-4-yl)aniline (28.4 mg, 0.32 mmol) (synthesized above) were mixed in a microwave vial with EtOH (1.5 mL). Then HCl (1 mL of a 0.1 M aq solution) was added to the tube, the tube was sealed, and the solution was heated to 150 °C for 40 min. The solvent was removed under reduced pressure and the residue washed with DCM and filtered to afford **9f** as a peach solid (90 mg, 72.0%). Mp: 160 °C dec. HPLC: 85.6% [t_R = 7.51 min, 30% CH_3OH in 0.1% TFA/water, 20 min]. ^{1}H NMR (400 MHz, methanol-d_4) δ 7.94 (s, 1H), 7.49 (d, J = 8.2 Hz, 2H), 7.35 (d, J = 8.4 Hz, 2H), 4.16 (p, J = 6.2 Hz, 1H), 3.86–3.68 (m, 2H), 3.65–3.46 (m, 4H), 3.22–3.09 (m, 2H), 3.00–2.90 (m, 1H), 2.14–1.82 (m, 8H), 1.69–1.58 (m, 1H). ^{13}C NMR (101 MHz, methanol-d_4) δ 159.20, 151.43, 141.84, 139.72, 135.04, 127.16, 122.99, 105.19, 76.74, 67.63, 45.23, 44.15, 39.15, 29.68, 28.54, 25.01. LC–MS (ESI+): *m/z* 388.18965 $(M + H)^+$. HRMS (ESI+): *m/z* calcd for $C_{20}H_{26}ClN_5O^+$ $(M + H)^+$ 388.1899, found 388.1900.

5-Bromo-*N*^{2}-(4-hydroxyphenyl)-*N*^{4}-[(tetrahydrofuran-2-yl)-methyl]pyrimidine-2,4-diamine Hydrochloride [(±)-9g]

A suspension of (±)-**8b** (0.073 g, 0.250 mmol) and 4-amino-2-chlorophenol (0.036 g, 0.250 mmol) in EtOH (1 mL) was heated in a microwave reactor at 150 °C for 20 min. The mixture was concentrated to dryness, EtOAc (3 mL) was then added, the resulting mixture

was sonicated for 5 min and filtered, and the precipitate was washed again with EtOAc (2 mL) and dried under high vacuum to afford the title compound as a gray solid (0.071 g, 65%). Mp: 193 °C dec. HPLC: 94.0% [t_R = 6.50 min, 45% CH_3OH in 0.1% TFA/water, 20 min]. ^{1}H NMR (400 MHz, CD_3OD): δ 7.96 (s, 1H), 7.51 (s, 1H), 7.15 (dd, J = 8.8, 2.4 Hz, 1H), 6.96 (d, J = 8.4 Hz, 1H), 4.18–4.11 (m, 1H), 3.86–3.80 (m, 1H), 3.76–3.71 (m, 1H), 3.56 (app d, J = 6.0 Hz, 2H), 2.05–1.97 (m, 1H), 1.93–1.86 (m, 2H), 1.65–1.56 (m, 1H). LC–MS (ESI+): *m/z* 399.02 and 401.02 for Br isotopes $(M + H)^+$. HRMS (ESI+): *m/z* calcd for $C_{15}H_{17}BrClN_4O_2$ $(M + H)^+$ 399.0218, found 399.0213.

5-Bromo-*N*^{2}-(4-morpholinophenyl)-*N*^{4}-[(tetrahydrofuran-2-yl)methyl]pyrimidine-2,4-diamine [(±)-9h]

A mixture of **8b** (0.100 g, 0.342 mmol) and 4-morpholinoaniline (0.067 g, 0.376 mmol) in EtOH (1 mL) was heated in a microwave reactor at 150 °C for 20 min. The precipitate was filtered, washed with ethyl acetate, and dried under high vacuum to afford the title compound **9h** as a white solid (0.115 mg, 65%). Mp: 198 °C dec. HPLC: 94.7% [t_R = 5.84 min, 45% CH_3OH in 0.1% TFA/water, 20 min]. ^{1}H NMR (400 MHz, CD_3OD): δ 7.98 (s, 1H), 7.46 (d, J = 8.4 Hz, 2H), 7.27 (d, J = 8.4 Hz, 2H), 4.19–4.13 (m, 1H), 3.92 (app t, J = 5.2 Hz, 4H), 3.86–3.80 (m, 1H), 3.76–3.71 (m, 1H), 3.61–3.56 (m, 2H), 3.35 (app t, J = 4.4 Hz, 4H), 2.04–1.87 (m, 3H), 1.67–1.59 (m, 1H). LC–MS (ESI+): *m/z* 434.13 $(M + H)^+$. HRMS (ESI+): *m/z* calcd for $C_{19}H_{25}BrN_5O_2$ $(M + H)^+$ 434.1186, found 434.1182.

Boc Derivative of 5-Bromo-*N*^{2}-[4-(piperazin-1-yl)phenyl]-*N*^{4}-[(tetrahydrofuran-2-yl)methyl]pyrimidine-2,4-diamine Hydrochloride [Intermediate for (±)-9i]

A mixture of **8b** (0.176 g, 0.6 mmol) and *tert*-butyl 4-(4-aminophenyl)piperazine-1-carboxylate (0.167 g, 0.6 mmol) in 2-propanol (3 mL) was heated at 80 °C in a sealed tube for 40 h (the reaction was monitored by HPLC–MS). The precipitate formed upon cooling the mixture was filtered, washed with 2-propanol (2 mL × 2), and dried under high vacuum to afford the title compound **9i** as a light green solid (0.300 g, 88%). Mp: 124 °C dec. HPLC: 98.5% [t_R = 7.51 min, 60% CH_3OH in 0.1% TFA/water, 20 min]. ^{1}H NMR (400 MHz, DMSO-d_6): δ 9.00 (s, 1H disappeared on D_2O shake), 7.94 (s, 1H), 7.53 (d, J = 8.8 Hz, 2H), 6.84 (d, J = 8.8 Hz, 2H), 6.76 (br t, J = 5.6 Hz, 1H, disappeared on D_2O shake), 4.10–4.03 (m, 1H), 3.78–3.73 (m, 1H), 3.63–3.58 (m, 1H), 3.43–3.40 (br m, 6H), 2.96 (t, J = 4.8 Hz, 4H), 1.90–1.77 (m, 3H), 1.62–1.56 (m, 1H), 1.40 (s, 9H). LC–MS (ESI+): *m/z* 533.19 and 535.19 for Br isotopes $(M + H)^+$. HRMS (ESI+): *m/z* calcd for $C_{24}H_{34}BrN_6O_3$ $(M + H)^+$ 533.1870, found 533.1862.

5-Bromo-*N*^{2}-[4-(piperazin-1-yl)phenyl]-*N*^{4}-[(tetrahydrofuran-2-yl)methyl]pyrimidine-2,4-diamine Trifluoroacetate Salt [(±)-9i]

To a solution of the Boc intermediate (0.291 g, 0.511 mmol) (synthesized in the above step) in DCM (2 mL) at 0 °C was added TFA (2 mL). The reaction mixture was warmed to rt and stirred for 1 h. The solvent was removed under reduced pressure. The resulting residue was slurried in DCM/EtOAc/hexane (1:1:2) and sonicated. The precipitate obtained was filtered, washed with EtOAc/hexane (1:1, 3 mL × 2), and dried under high vacuum to afford the title compound **9i** as a gray solid (0.340 g, 98%). Mp: 200 °C dec. HPLC: 100% [t_R = 4.28 min,

35% CH_3OH in 0.1% TFA/water, 20 min]. ^1H NMR (400 MHz, DMSO-d_6): δ 9.50 (br s, 1H, disappeared on D_2O shake), 8.76 (s, 1H, disappeared on D_2O shake), 8.04 (s, 1H), 7.49 (d, J = 8.80 Hz, 2H), 6.92 (d, J = 8.85 Hz, 2H), 4.08–4.03 (m, 1H), 3.74–3.70 (m, 1H), 3.62–3.57 (m, 1H), 3.41 (t, J = 6.4 Hz, 2H), 3.24–3.22 (m, 8H), 1.91–1.74 (m, 3H), 1.61–1.54 (m, 1H). ^{19}F NMR (376 MHz, DMSO-d_6): δ –74.19 (s). LC–MS (ESI+): *m/z* 433.12 and 435.12 for Br isotopes $(M + H)^+$. HRMS (ESI+): *m/z* calcd for $C_{19}H_{26}BrN_6O$ $(M + H)^+$ 433.1346, found 433.1335.

5-Bromo-*N*^{2}-{4-[(4-carboxyethyl)piperidinyl]phenyl}-*N*^{4}-[(tetrahydrofuran-2-yl)methyl]pyrimidine-2,4-diamine [Intermediate for (±)-9j]

A mixture of **8b** (0.200 g, 0.683 mmol) and ethyl 1-(4-aminophenyl)piperidine-4-carboxylate (0.186 g, 0.752 mmol) in EtOH (2 mL) was heated in a microwave reactor at 150 °C for 20 min. The precipitate obtained was filtered, washed with ethyl acetate, and dried under high vacuum to afford the title compound as a brown solid (0.070 mg, 22%). Mp: 137 °C dec. HPLC: 99.7% [t_R = 6.55 min, 45% CH_3OH in water (0.1% TFA), 20 min]. ^1H NMR (400 MHz, DMSO) δ 8.96 (s, 1H), 7.94 (s, 1H), 7.50 (d, J = 8.8 Hz, 2H), 6.80 (d, J = 8.8 Hz, 2H), 6.74 (t, J = 6.4 Hz, 1H), 4.05 (q, J = 6.8 Hz, 2H), 3.75 (q, J = 7.6 Hz, 1H), 3.60 (q, J = 7.2 Hz, 1H), 3.49–3.88 (m, 5H), 2.64 (t, J = 11.2 Hz, 2H), 2.45–2.33 (m, 1H), 1.89–1.79 (m, 4H), 1.73–1.60 (m, 2H), 1.17 (t, J = 7.2, 3H). LC–MS (ESI+): *m/z* 503.2 $(M + H)^+$. HRMS (ESI+): *m/z* calcd for $C_{23}H_{30}BrN_5O_3$ $(M + H)^+$ 504.1605, found 504.1597.

5-Bromo-*N*^{2}-[4-(4-carboxypiperidinyl)phenyl]-*N*^{4}-[(tetrahydrofuran-2-yl)methyl]pyrimidine-2,4-diamine [(±)-9j]

The ester intermediate (0.025 g, 0.050 mmol) (synthesized above) in THF (0.248 mL) and 2 M NaOH (0.200 mL) were stirred at room temperature for 18 h. The resulting solution was concentrated, and the product obtained was dissolved in water (2 mL). The aqueous solution was acidified with 1 M HCl to pH 4–5, and the solid mixture obtained was filtered to afford **9j** as a pure light brown solid (0.019 g, 81%). Mp: 129–133 °C. HPLC: 99.7% [t_R = 6.55 min, 45% CH_3OH in water (0.1% TFA), 20 min]. ^1H NMR (400 MHz, DMSO) δ 12.19 (s, 1H), 8.95 (s, 1H), 7.93 (s, 1H), 7.49 (d, J = 9.2 Hz, 2H), 6.81 (d, J = 8.8 Hz, 2H), 6.74 (t, J = 5.6 Hz, 1H), 4.09–4.03 (m, 1H), 3.78–3.73 (m, 1H), 3.63–3.57 (m, 2H), 3.45 (dt, J = 12.4, 3.2 Hz, 1H), 3.42–3.39 (m, 1H), 2.61 (t, J = 9.2 Hz, 2H), 2.35–2.30 (m, 1H), 1.89–1.73 (m, 5H), 1.67–1.53 (m, 2H). LC–MS (ESI+): *m/z* 476.12 $(M + H)^+$. HRMS (ESI+): *m/z* calcd for $C_{21}H_{26}BrN_5O_3$ (M + H) 476.1292, found 476.1285.

5-Bromo-*N*^{2}-[4-(piperidin-4-yl)phenyl]-*N*^{4}-[(tetrahydrofuran-2-yl)methyl]pyrimidine-2,4-diamine [(±)-9k]

A mixture of **8b** (0.047 g, 0.161 mmol) and 4-(piperidin-4-yl)aniline (0.028 g, 0.161 mmol) (synthesis described above) in EtOH (1 mL) and HCl (1 mL, 0.1 M aq solution) was heated in a microwave reactor at 150 °C for 40 min. The solvent was removed, and the residue was slurried with DCM, filtered, and dried under high vacuum to afford the title compound **9k** as a white solid (0.014 mg, 19%). Mp: 162 °C dec. HPLC: 98.8% [t_R = 2.50 min, 45% CH_3OH in 0.1% TFA/water, 20 min]. ^1H NMR (400 MHz, CD_3OD): δ 8.01 (s, 1H), 7.47 (d, J = 8.0

Hz, 2H), 7.37 (d, *J* = 8.4 Hz, 2H), 4.18–4.12 (m, 1H), 3.83–3.76 (m, 1H), 3.75–3.69 (m, 1H), 3.59–3.49 (m, 4H), 3.15 (t, *J* = 12.8 Hz, 2H), 2.96 (t, *J* = 7.2 Hz, 1H), 2.10–1.87 (m, 7H), 1.66–1.58 (m, 1H). LC–MS (ESI+): *m/z* 432.13; $(M + H)^+$. HRMS (ESI+): *m/z* calcd for $C_{20}H_{27}N_5O$ $(M + H)^+$ 432.1394, found 432.1392.

5-[(2-Chloro-6-fluorophenyl)carbamoyl]-*N*^{2}-{4-[(4-carboxyethyl)piperidinyl]phenyl}-*N*^{4}-[(tetrahydrofuran-2-yl)methyl]pyrimidine-2,4-diamine [Intermediate for (±)-9l]

A mixture of **8c** (0.200 g, 0.519 mmol) and ethyl 1-(4-aminophenyl)piperidine-4-carboxylate (0.141 g, 0.571 mmol) in EtOH (2 mL) was heated in a microwave reactor at 150 °C for 20 min. The resulting precipitate was filtered, washed with ethyl acetate, and dried under high vacuum to afford the title compound as a gray solid (0.215 mg, 71%). Mp: 137–141 °C. HPLC: 94.1% [t_R = 12.01 min, gradient 5–95% CH_3OH in water (0.1% formic acid), 20 min]. ^{1}H NMR (400 MHz, DMSO) δ 7.86 (s, 1H), 7.44 (d, *J* = 9.2 Hz, 2H), 6.95 (d, *J* = 9.2 Hz, 2H), 4.14 (q, *J* = 7.2 Hz, 3H), 3.88–3.86 (m, 1H), 3.77–3.72 (m, 1H), 3.62–3.44 (m, 4H), 2.73 (dt, *J* = 11.6, 2.4 Hz, 2H), 2.54–2.41 (m, 1H), 2.03–1.78 (m, 7H), 1.69–1.62 (m, 1H), 1.26 (t, *J* = 7.2 Hz, 3H). LC–MS (ESI+): *m/z* 597.21 $(M + H)^+$. HRMS (ESI+): *m/z* calcd for $C_{30}H_{37}ClFN_6O_4$ $(M + H)^+$ 597.2388, found 597.2378.

5-[(2-Chloro-6-fluorophenyl)carbamoyl]-*N*^{2}-[4-(4-carboxypiperidinyl)phenyl]-*N*^{4}-[(tetrahydrofuran-2-yl)methyl]pyrimidine-2,4-diamine [(±)-9l]

The ester intermediate (0.100 g, 0.167 mmol) synthesized above in THF (1 mL) and 2 M NaOH (0.200 mL) were stirred at room temperature for 18 h. The resulting solution was concentrated, and the product obtained was dissolved in water (2 mL). The aqueous solution was acidified with HCl (1 M aq solution) to pH 4–5, and the solid mixture obtained was filtered to afford **9j** as a white solid (0.75 mg, 78%). Mp: 145.1 °C. HPLC: 99.3% [t_R = 4.20 min, 55% CH_3OH in 0.1% TFA/water, 20 min]. ^{1}H NMR (400 MHz, DMSO-d_6): δ 12.23 (s, 1H), 9.84 (s, 1H), 9.49 (br s, 1H), 8.85 (br s, 1H), 8.73 (s, 1H), 7.57 (d, *J* = 7.6 Hz, 2H), 7.43–7.30 (m, 3H), 6.87 (d, *J* = 7.6 Hz, 2H), 4.01–3.98 (m, 1H), 3.76–3.71 (m, 1H), 3.62–3.50 (m, 4H), 3.43–3.38 (m, 1H), 2.66 (app t, 2H), 2.34 (app t, 1H), 1.94–1.77 (m, 5H), 1.67–1.48 (m, 3H). LC–MS (ESI+): *m/z* 569.2 $(M + H)^+$. HRMS (ESI+): *m/z* calcd for $C_{28}H_{31}ClFN_6O_4$ $(M + H)^+$ 569.2074, found 569.2063.

Boc Derivative of 5-[(2-Chloro-6-fluorophenyl)carbamoyl]-*N*^{2}-[4-(piperazin-1-yl]phenyl]-*N*^{4}-[(tetrahydrofuran-2-yl)-methyl]pyrimidine-2,4-diamine [Intermediate for (±)-9m]

A mixture of **8c** (0.308 g, 0.8 mmol) and *tert*-butyl 4-(4-aminophenyl)piperazine-1-carboxylate (0.222 g, 0.8 mmol) in 2-propanol (4 mL) was heated at 80 °C in a sealed tube for 5 h. The resulting precipitate was filtered upon cooling, washed with 2-propanol (2 mL × 3), and then dried under vacuum to afford the title compound as a light green solid (0.440 g, 83%). Mp: 184–186 °C. HPLC: 99.8% [t_R = 5.23 min, 70% CH_3OH in 0.1% TFA/water, 20 min]. ^{1}H NMR (400 MHz, DMSO-d_6): δ 10.26 (br s, 1H, disappeared on D_2O shake), 10.12 (br s, 1H, disappeared on D_2O shake), 9.31 (br s, 1H, disappeared on D_2O shake), 8.71 (s, 1H), 7.51–7.33 (m, 4H), 7.02 (app d, *J* = 6.0 Hz, 2H), 4.05–3.98 (m, 1H), 3.75–3.70 (m, 1H, overlapping with water peak), 3.63–3.57 (m, 1H, overlapping with water peak), 3.47–3.42 (m, 6H), 3.10 (br s, 4H), 1.93–1.88 (m, 1H), 1.83–1.76 (m, 2H), 1.56–1.48 (m, 1H), 1.40 (s,

9H). ^{19}F NMR (376 MHz, DMSO-d_6): δ –116.16 to –116.20 (m). LC–MS (ESI+): *m/z* 626.25 $(M + H)^+$. HRMS (ESI+): *m/z* calcd for $C_{31}H_{38}ClFN_7O_4$ $(M + H)^+$ 626.2652, found 626.2651.

5-[(2-Chloro-6-fluorophenyl)carbamoyl]-*N*^{2}-[(4-piperazin-1-yl]phenyl]-*N*^{4}-[(tetrahydrofuran-2-yl)methyl]pyrimidine-2,4-diamine Trifluoroacetate Salt [(±)-9m]

To a solution of the Boc intermediate synthesized above (0.408 g, 0.616 mmol) in DCM (4 mL) at 0 °C was added TFA (4 mL). The reaction mixture was warmed to rt and stirred for 1 h. The solvent was removed under reduced pressure. The resulting residue was slurried in EtOAc/hexane (1:2) and sonicated. The precipitate was filtered, washed with EtOAc/hexane (1:1) (3 mL × 2), and dried under high vacuum to afford the title compound as a gray solid (0.400 g, 102%). Mp: 205 °C dec. HPLC: 99.5% [t_R = 4.44 min, 50% CH_3OH in 0.1% TFA/water, 20 min]. ^{1}H NMR (400 MHz, DMSO-d_6): δ 9.99 (s, 1H, disappeared on D_2O shake), 9.80 (br s, 1H, disappeared on D_2O shake), 9.04 (br s, 1H, disappeared on D_2O shake) 8.73 (s, 1H), 7.60 (d, *J* = 8.8 Hz, 2H), 7.44–7.31 (m, 3H), 6.96 (d, *J* = 8.8 Hz, 2H), 4.04–3.98 (m, 1H), 3.74–3.72 (m, 1H), 3.63–3.58 (m, 2H), 3.44–3.39 (m, 1H), 3.27–3.23 (m, 8H), 1.94–1.88 (m, 1H), 1.83–1.77 (m, 2H), 1.57–1.49 (m, 1H). ^{19}F NMR (376 MHz, DMSO-d_6): δ –74.24 (s, 3H), –116.17 to –116.21 (m, 1H). LC–MS (ESI+): *m/z* 526.22 $(M + H)^+$. HRMS (ESI+): *m/z* calcd for $C_{26}H_{30}ClFN_7O_2$ $(M + H)^+$ 526.2128, found 526.2123.

5-[(2-Chloro-6-fluorophenyl)carbamoyl]-*N*^{2}-[(4-morpholinophenyl]-*N*^{4}-[(tetrahydrofuran-2-yl)methyl]pyrimidine-2,4-diamine [(±)-9n]

The chloropyrimidine **8c** (100 mg, 0.26 mmol) and 4-morpholinoaniline (0.069 g, 0.38 mmol) were mixed in a microwave tube with HCl (110 μL of a 4 M solution in dioxane). 2-Methoxyethanol (4.00 mL) was added to the mixture and the resulting mixture heated at 110 °C for 16 h. The resulting solution was concentrated, and the product was partitioned between $CHCl_3$ and saturated aqueous $NaHCO_3$. The organic phase was then dried over Na_2SO_4, filtered, and concentrated. The resulting solid was slurried twice with dichloromethane and hexane, filtered, and dried under reduced pressure to yield **9n** as a light green solid (0.080 g). Mp: 231 °C dec. ^{1}H NMR (400 MHz, CD_3OD): 8.50 (s, 1H), 7.38–7.37 (m, 4H), 7.24–7.19 (m, 1H), 7.08 (d, *J* = 8.8 Hz, 2H), 4.16–4.10 (m, 1H), 3.85 (t, *J* = 4.8 Hz, 4H), 3.76–3.59 (m, 3H), 3.20 (t, *J* = 4.8 Hz, 5H), 2.01–1.91 (m, 3H), 1.66–1.58 (m, 1H). HPLC–MS (ESI+): *m/z* 527.2 (100%). HRMS (ESI+): *m/z* calcd for $C_{27}H_{31}ClFN_6O_3$ (M + H) 527.1968, found 527.1962.

5-[(2-Chloro-6-fluorophenyl)carbamoyl]-*N*^{2}-[(4-(piperidin-4-yl)phenyl]-*N*^{4}-[(tetrahydrofuran-2-yl)methyl]pyrimidine-2,4-diamine [(±)-9o]

A mixture of chloropyrimidine **8c** (0.062 g, 0.161 mmol) and 4-piperidinylaniline (0.028 g, 0.161 mmol) in EtOH (1 mL) and HCl (1 mL of a 0.1 M aq solution) was heated in a microwave reactor at 150 °C for 40 min. The solvent was removed, and the resulting residue was slurried with DCM, filtered, and dried under high vacuum to afford the title compound **9o** as a solid (0.032 mg, 36%). Mp: 186 °C dec. HPLC: 89.4% [t_R = 10.37 min, 45% CH_3OH in 0.1% TFA/water, 20 min]. ^{1}H NMR (400 MHz, CD_3OD): δ 8.60 (d, *J* = 4.0 Hz, 1H), 7.55 (d, *J* = 7.6 Hz, 2H), 7.40–7.38 (m, 3H),), 7.25–7.19 (m, 1H), 4.19–4.10 (m, 1H),

3.93–3.80 (m, 1H), 3.75–3.60 (m, 3H), 3.53–3.50 (d, *J* = 12.0 Hz, 2H), 3.16 (t, *J* = 10.4 Hz, 2H), 2.97 (t, *J* = 12.0 Hz, 1H), 2.11–1.89 (m, 6H), 1.67–1.60 (m, 1H). LC–MS (ESI+): *m/z* 525.2; $(M + H)^+$. HRMS (ESI+): *m/z* calcd for $C_{27}H_{31}ClFN_6O_2$ $(M + H)^+$ 525.2176, found 525.2175.

5-[(2-Chloro-6-fluorophenyl)carbamoyl]-*N*^{2}-[(3-fluoro-4-hydroxyphenyl)amino]-*N*^{4}-[(tetrahydrofuran-2-yl)methyl]pyrimidine-2,4-diamine [(±)-9p]

This compound was synthesized according to the procedure described for **9o** using **8c** (0.050 g, 0.130 mmol), 4-amino-2-fluorophenol (0.017 g, 0.130 mmol), and EtOH (1 mL). A mixture of EtOAc/hexane was used for recrystallization to afford the title compound as a brown solid (0.051 g, 76%). Mp: 183 °C dec. HPLC: 99.4% [t_R = 6.53 min, 55% CH_3OH in 0.1% TFA/water, 20 min]. ^{1}H NMR (400 MHz, CD_3OD): δ 8.54 (s, 1H), 7.43–7.38 (m, 3H), 7.24–7.19 (m, 1H), 7.10 (d, *J* = 8.4 Hz, 1H), 6.96 (t, *J* = 8.4 Hz, 1H), 4.15–4.09 (m, 1H), 3.90–3.85 (m, 1H), 3.77–3.59 (m, 3H), 2.05–1.99 (m, 1H), 1.96–1.88 (m, 1H), 1.67–1.58 (m, 1H). ^{19}F NMR (376 MHz, CD_3OD): δ –118.25 (d). LC–MS (ESI+): *m/z* 476.12 $(M + H)^+$. HRMS (ESI+): *m/z* calcd for $C_{22}H_{21}F_2N_5O_3$ $(M + H)^+$ 476.1296, found 476.1290.

5-[(2-Chloro-6-fluorophenyl)carbamoyl]-*N*^{2}-[(4-methoxyphenyl)amino]-*N*^{4}-[(tetrahydrofuran-2-yl)methyl]pyrimidine-2,4-diamine [(±)-9q]

A mixture of **8c** (0.050 g, 0.130 mmol), 4-methoxyaniline (0.016 g, 0.132 mmol), and HCl (0.033 mL of a 4 M solution in dioxane, 0.132 mmol) in dioxane (1 mL) was heated in a microwave reactor at 180 °C for 30 min. The mixture was evaporated to dryness, EtOAc was added (5 mL), and the resulting mixture was sonicated. The resulting solid was filtered, washed with satd $NaHCO_3$ (5 mL × 2) and water (5 mL × 2), and dried under vacuum to afford the title compound **9q** as a pure white solid (0.051 g, 84%). Mp: 201 °C dec. HPLC: 99.5% [t_R = 4.37 min, 65% CH_3OH in 0.1% TFA/water, 20 min]. ^{1}H NMR (400 MHz, DMSO-d_6): δ 10.22 (s, 1H), 10.06 (br s, 1H), 9.27 (br s, 1H), 8.72 (s, 1H), 7.54 (app d, *J* = 7.6 Hz, 2H), 7.45–7.32 (m, 3H), 6.93 (d, *J* = 8.8 Hz, 2H), 4.04–3.98 (m, 1H), 3.75–3.70 (m, 4H), 3.61–3.55 (m, 3H), 1.95–1.87 (m, 1H), 1.82–1.76 (m, 2H), 1.56–1.48 (m, 1H). ^{19}F NMR (376 MHz, DMSO-d_6): δ –116.16 to –116.19 (m). LC–MS (ESI+): *m/z* 472.14 $(M + H)^+$. HRMS (ESI+): *m/z* calcd for $C_{23}H_{24}ClFN_5O_3$ $(M + H)^+$ 472.1546, found 472.1548.

5-[(2-Chloro-6-fluorophenyl)carbamoyl]-*N*^{2}-[(4-hydroxyphenyl)amino]-*N*^{4}-[(tetrahydrofuran-2-yl)methyl]pyrimidine-2,4-diamine [(±)-9r]

This compound was synthesized using the procedure described for **9q** using pyrimidine **8c** (0.050 g, 0.130 mmol) and 4-aminophenol (0.017 g, 0.156 mmol) to obtain the title compound **9r** as a beige solid (0.046 g, 78%). Mp: 263 °C dec. HPLC: 99.4% [t_R = 6.77 min, 55% CH_3OH in 0.1% TFA/water, 20 min]. ^{1}H NMR (400 MHz, DMSO-d_6): δ 9.82 (s, 1H), 9.41 (br s, 1H), 9.09 (s, 1H), 8.83 (br s, 1H), 8.72 (s, 1H), 7.49 (d, *J* = 8.4 Hz, 2H), 7.43–7.30 (m, 3H), 6.67 (d, *J* = 8.8 Hz, 2H), 4.02–3.98 (m, 1H), 3.76–3.71 (m, 1H), 3.62–3.57 (m, 2H), 3.42–3.37 (m, 1H), 1.93–1.87 (m, 1H), 1.84–1.75 (m, 2H), 1.56–1.47 (m, 1H). ^{19}F NMR (376 MHz, DMSO-d_6): δ –116.15 to –116.19 (m). LC–MS (ESI+): *m/z* 458.13 $(M + H)^+$. HRMS (ESI+): *m/z* calcd for $C_{22}H_{22}ClFN_5O_3$ $(M + H)^+$ 458.1390, found 458.1390.

5-Fluoro-*N*^{2}-[(4-hydroxy-3-fluorophenyl)amino]-*N*^{4}-[(tetrahydrofuran-2-yl)methyl]pyrimidine-2,4-diamine Hydrochloride [(±)-9s]

A mixture of pyrimidine **8d** (0.116 g, 0.5 mmol) and 4-amino-2-fluorophenol (0.064 g, 0.5 mmol) in EtOH (2 mL) was heated in a microwave reactor at 150 °C for 20 min. The solvent was removed, and the resulting residue was slurried and sonicated with EtOAc (3 mL). The mixture was filtered, and the precipitate was washed with EtOAc (2 mL) and then dried under high vacuum to afford the title compound as a dark brown solid (0.152 g, 84%). Mp: 201 °C dec. HPLC: 98.5% [t_R = 7.72 min, 35% CH_3OH in 0.1% TFA/water, 20 min]. ^{1}H NMR (400 MHz, DMSO-d_6): δ 10.23 (s, 1H), 9.87 (br s, 1H), 10.18 (s, 1H), 9.19 (br s, 1H), 8.08 (d, J = 5.2 Hz, 1H), 7.43 (dd, J = 13.2, 2.0 Hz, 1H), 7.01 (dd, J = 8.8, 1.6 Hz, 1 H), 6.94 (t, J = 9.6 Hz, 1H), 4.07–4.01 (m, 1H), 3.75–3.69 (m, 1H), 3.63–3.58 (m, 1H), 1.93–1.85 (m, 1H), 1.83–1.75 (m, 2H), 1.59–1.51 (m, 1H). ^{19}F NMR (376 MHz, DMSO-d_6): δ –134.70 (s), –163.23 (s). LC–MS (ESI+): *m/z* 323.14 $(M + H)^+$. HRMS (ESI+): *m/z* calcd for $C_{15}H_{17}F_2N_4O_2$ $(M + H)^+$ 323.1314, found 323.1314.

5-Methyl-*N*^{2}-[(4-hydroxy-3-fluorophenyl)amino]-*N*^{4}-[(tetrahydrofuran-2-yl)methyl]pyrimidine-2,4-diamine Hydrochloride [(±)-9t]

A suspension of pyrimidine **8e** (0.114 g, 0.5 mmol) and 4-amino-2-fluorophenol (0.064 g, 0.5 mmol) in EtOH (1 mL) was heated in a microwave reactor at 150 °C for 20 min. The mixture was concentrated, and the residue obtained was recrystallized with MeOH/EtOAc, filtered, and washed with EtOAc (2 mL) to afford the title compound **9t** as a dark brown solid. The filtrate was concentrated and recrystallized again with MeOH/EtOAc to afford a second crop of solid. The solids were combined to afford the title compound **9t** as a dark brown solid (0.163 g, 92%). Mp: 199 °C dec. HPLC: 98.8% [t_R = 12.26 min, 35% CH_3OH in 0.1% TFA/water, 20 min]. ^{1}H NMR (400 MHz, CD_3OD): δ 7.45 (s, 1H), 7.29 (dd, J = 12.0, 1.6 Hz, 1H), 7.03–6.93 (m, 2H), 4.20–4.13 (m, 1H), 3.88–3.83 (m, 1H), 3.78–3.72 (m, 1H), 3.64–3.51 (m, 2H), 2.04 (s, 3H), 1.96–1.87 (m, 2H), 1.66–1.57 (m, 1H). ^{19}F NMR (376 MHz, CD_3OD): δ –136.94 (s). LC–MS (ESI+): *m/z* 319.16 $(M + H)^+$. HRMS (ESI+): *m/z* calcd for $C_{16}H_{20}FN_4O_2$ $(M + H)^+$ 319.1565, found 319.1566.

5-Bromo-*N*^{2}-[(4-hydroxy-3-fluorophenyl)amino]-*N*^{4}-[(tetrahydrofuran-2-yl)methyl]pyrimidine-2,4-diamine [(±)-13]

A mixture of pyrimidine **8b** (0.400 g, 1.4 mmol) and 4-amino-2-fluorophenol (0.174 g, 1.4 mmol) in EtOH (3 mL) in a microwave vial was heated to 150 °C for 20 min in a microwave reactor. The solvent was evaporated, and the residue obtained was washed with ethyl acetate, slurried with dichloromethane and hexane, and filtered to afford **13** as a pure beige solid (0.580 g, 98%). Mp: 205–207 °C. HPLC: 94% [t_R = 6.33 min, 40% CH_3OH in 0.1% TFA/water, 20 min]. ^{1}H NMR (400 MHz, DMSO-d_6): δ 10.20 (s, 1H), 9.83 (br s, 1H), 8.34 (br s, 1H), 8.16 (s, 1H), 7.44 (dd, J = 12.8, 2.0 Hz, 1H), 7.02 (dd, J = 8.4, 1.2 Hz, 1H), 6.91 (t, J = 8.4 Hz, 1H), 4.07–4.01 (m, 1H), 3.72–3.67 (m, 1H), 3.60–3.55 (m, 1H), 3.42–3.37 (m, 2H), 1.88–1.71 (m, 3H), 1.56–1.48 (m, 1H). HPLC–MS (ESI+): *m/z* 383 and 385 for Br isotopes $(M + H)^+$. HRMS (ESI+): *m/z* calcd for $C_{15}H_{17}BrFN_4O_2$ $(M + H)^+$ 383.0513, found 383.0513.

5-[(2-Chloro-6-fluorophenyl)carbamoyl]-*N*^{2}-(3-fluoro-4-hydroxyphenyl)-*N*^{4}-[(tetrahydrofuran-2-yl)methyl]pyrimidine-2,4-diamine Hydrochloride [(±)-14]

This compound was synthesized using the procedure described for **9t** except using **8c** (0.050 g, 0.130 mmol), 4-amino-2-fluorophenol (0.017 g, 0.130 mmol), and EtOH (1 mL). EtOAc/hexane was used for recrystallization to afford the title compound as a brown solid (0.051 g, 76%). Mp: 183 °C dec. HPLC: 99.4% [t_R = 6.53 min, 55% CH_3OH in 0.1% TFA/water, 20 min]. ^{1}H NMR (400 MHz, CD_3OD): δ 8.54 (s, 1H), 7.43–7.38 (m, 3H), 7.24–7.19 (m, 1H), 7.10 (d, *J* = 8.4 Hz, 1H), 6.96 (t, *J* = 8.4 Hz, 1H), 4.15–4.09 (m, 1H), 3.90–3.85 (m, 1H), 3.77–3.59 (m, 3H), 2.05–1.99 (m, 1H), 1.96–1.88 (m, 2H), 1.67–1.58 (m, 1H). ^{19}F NMR (376 MHz, CD_3OD): δ –118.25 (d). LC–MS (ESI+): *m/z* 476.12 $(M + H)^+$. HRMS (ESI+): *m/z* calcd for $C_{22}H_{21}F_2N_5O_3$ $(M + H)^+$ 476.1296, found 476.1290.

5-Chloro-*N*^{2}-(4-hydroxyphenyl)-*N*^{4}-[(tetrahydrofuran-2-yl)-methyl]pyrimidine-2,4-diamine Hydrochloride [(±)-15]

A mixture of **8a** (0.050 g, 0.20 mmol) and 4-aminophenol (0.024 g, 0.22 mmol) in EtOH (0.500 mL) in a microwave vial was heated to 150 °C for 20 min in a microwave reactor. The precipitate formed upon cooling the mixture was filtered, washed with ethyl acetate, slurried with dichloromethane and hexane, and filtered to afford **15** as a brown solid (0.027 g, 42%). Mp: 214.0 °C dec. HPLC: 100% [t_R = 8.90 min, gradient 5–95% CH_3OH in water (0.1% formic acid), 20 min]. ^{1}H NMR (400 MHz, DMSO-d_6) δ 9.85 (s, 1H), 9.43 (s, 1H), 8.45 (s, 1H), 8.03 (s, 1H) 7.27 (d, *J* = 8.8 Hz, 2H), 6.74 (d, *J* = 8.8 Hz, 2H), 4.08–4.01 (m, 1H), 3.73–3.68 (m, 1H), 3.62–3.57 (m, 2H), 1.90–1.74 (m, 3H), 1.58–1.50 (m, 1H). LC–MS (ESI+): *m/z* 320.10400 $(M + H)^+$. HRMS (ESI+): *m/z* calcd for $C_{15}H_{17}ClN_4O_2$ (M + H) 321.11128, found 321.11161.

5-Bromo-*N*^{2}-(4-hydroxyphenyl)-*N*^{4}-[(tetrahydrofuran-2-yl)methyl]pyrimidine-2,4-diamine Hydrochloride [(±)-16]

A mixture of **8b** (0.500 g, 1.7 mmol) and 4-aminophenol (0.186 g, 1.7 mmol) in EtOH (5 mL) in a microwave vial was heated to 150 °C for 20 min in a microwave reactor. The solvent was evaporated, and the residue obtained was filtered, washed with ethyl acetate, slurried with dichloromethane and hexane, and filtered to afford **16** as a gray solid (0.70 g, 99%). Mp: 188 °C dec. HPLC: 95.7% [t_R = 5.83 min, 40% CH_3OH in water (0.1% TFA), 20 min]. ^{1}H NMR (400 MHz, CD3OD): δ 7.90 (s, 1H), 7.22 (d, *J* = 8.4 Hz, 2H), 6.85 (d, *J* = 8.4 Hz, 2H), 4.16–4.13 (m, 1H), 3.84–3.82 (m, 1H), 3.76–3.71 (m, 1H), 3.56 (d, *J* = 5.6 Hz, 2H), 2.01–1.89 (m, 3H), 1.63–1.58 (m, 1H). LC–MS (ESI+): *m/z* 367 $(M + H)^+$. HRMS (ESI+): *m/z* calcd for $C_{15}H_{17}BrN_4O_2$ (M + H) 365.0607, found 365.0586.

5-Bromo-*N*^{2}-(4-hydroxy-3-methylphenyl)-*N*^{4}-[(tetrahydrofuran-2-yl)methyl]pyrimidine-2,4-diamine Hydrochloride [(±)-17]

A mixture of **8b** (0.400 g, 1.4 mmol) and 4-aminophenol (0.168 g, 1.4 mmol) in EtOH (3 mL) in a microwave vial was heated to 150 °C for 20 min in a microwave reactor. The solvent was evaporated, and the residue obtained was washed with ethyl acetate, slurried with dichloromethane and hexane, and filtered to afford **17** as a pure gray solid (0.60 g, 99%). Mp: 206–209 °C. HPLC: 96% [t_R = 5.64 min, 45% CH_3OH in 0.1% TFA/water, 20

min] ^{1}H NMR (400 MHz, CD_3OD): δ 7.86 (s, 1H), 7.11 (s, 1H), 7.03 (d, J = 8.0 Hz, 1H), 6.80 (d, J = 8.4 Hz, 1H), 4.18–4.13 (m, 1H), 3.86–3.82 (m, 1H), 3.76–3.71 (m, 1H), 3.57 (d, J = 5.6 Hz, 2H), 2.20 (s, 3H), 2.01–1.90 (m, 3H), 1.65–1.57 (m, 1H). LC–MS (ESI+): *m/z* 367 $(M + H)^+$. HRMS (ESI+): *m/z* calcd for $C_{16}H_{20}BrN_4O_2$ (M + H) 379.0764, found 379.0760.

5-Bromo-*N*^{2}-(4-methoxyphenyl)-*N*^{4}-[(tetrahydrofuran-2-yl)methyl]pyrimidine-2,4-diamine Hydrochloride [(±)-18]

A mixture of **8b** (0.100 g, 0.34 mmol) and 4-methoxyaniline (0.040 g, 0.34 mmol) in EtOH (2 mL) in a microwave vial was heated to 150 °C for 20 min in a microwave reactor. The solvent was evaporated, and the residue obtained was washed with ethyl acetate, slurried with dichloromethane and hexane, and filtered to afford **18** as a brown solid (0.134 g, 93%). Mp: 192 °C dec. HPLC: 95.6% [t_R = 9.89 min, 45% CH_3OH in water (0.1% TFA), 20 min]. ^{1}H NMR (400 MHz, DMSO-d_6): δ 7.91 (s, 1H), 7.34 (d, J = 8.8 Hz, 2H), 6.99 (d, J = 8.8 Hz, 2H), 4.16–4.13 (m, 1H), 3.87–3.79 (m, 4H), 3.82 (s, 3H), 3.56 (d, J = 5.6 Hz, 2H), 2.00–1.88 (m, 3H), 1.65–1.59 (m, 1H). LC–MS (ESI+): *m/z* 379 and 381 for Br isotopes $(M + H)^+$. HRMS (ESI+): *m/z* calcd for $C_{16}H_{19}BrN_4O_2$ (M + H) 379.0764, found 379.0766.

5-Bromo-*N*^{2}-[4-(4-methylpiperazin-1-yl)phenyl]-*N*^{4}-[(tetrahydrofuran-2-yl)methyl]pyrimidine-2,4-diamine [(±)-19]

The piperazine **9i** (0.055 g, 0.10 mmol), iodomethane (0.014 g, 0.10 mmol), and potassium carbonate (0.55 g, 0.40 mmol) were mixed in MeOH (2 mL) and stirred at room temperature for 8 h. The mixture was then concentrated under reduce pressure, and the solid was purified by flash chromatography (5 g of silica gel, 0–5% MeOH) to afford **19** as a yellow solid (0.012 g, 27%). Mp: 123 °C dec. ^{1}H NMR (400 MHz, DMSO-d_6) δ 8.97 (s, 1H), 7.94 (s, 1H), 7.54 (d, J = 8.8 Hz, 2H), 6.83 (d, J = 8.8 Hz, 2H), 6.75 (t, J = 5.6 Hz, 1H), 4.08–4.03 (m, 1H), 3.78–3.73 (m, 1H), 3.63–3.58 (m, 1H), 3.43–3.40 (m, 2H), 3.05 (br s, 4H), 2.54 (br s, 4H, partially overlapped with DMSO signal), 2.29 (s, 3H), 1.91–1.56 (m, 3H), 1.63–1.56 (m, 1H). LC–MS (ESI+): *m/z* 446.14297 $(M + H)^+$. HRMS (ESI+): *m/z* calcd for $C_{15}H_{17}ClN_4O_2$ (M + H) 447.1502, found 447.1493.

5-[(2-Chloro-6-fluorophenyl)carbamoyl]-*N*^{2}-[4-(4-methylpiperazin-1-yl)phenyl]-*N*^{4}-[(tetrahydrofuran-2-yl)methyl]pyrimidine-2,4-diamine [(±)-20]

The chloropyrimidine **8c** (0.150 g, 0.390 mmol) and 4-(4-methylpiperazin-1-yl)aniline (0.082 g, 0.430 mmol) were mixed in a microwave vial with HCl (110 μL of 4 M solution in dioxane). 2-Methoxyethanol (4.00 mL) was added to the mixture, and the resulting solution was heated at 110 °C for 16 h. The resulting solution was concentrated under reduced pressure, and the product was partitioned between $CHCl_3$ and saturated aqueous $NaHCO_3$. The organic phase was then dried (Na_2SO_4), filtered, and concentrated under reduced pressure. The resulting solid was slurried twice with dichloromethane and hexane, filtered, and dried under reduced pressure to yield **20** as a dark gray solid (0.097 g, 47%). Mp: 210.4 °C dec. HPLC: 90.8% [t_R = 10.2 min, gradient 5–95% CH_3OH in water (0.1% formic acid), 20 min]. ^{1}H NMR (400 MHz, DMSO) δ 9.83 (s, 1H), 9.46 (s, 1H), 8.85 (s, 1H), 8.73 (s, 1H), 7.598 (d, J = 8.8 Hz, 2H), 7.43–7.30 (m, 3H), 6.86 (d, J = 8.8 Hz, 2H), 4.01–3.90 (m,

1H), 3.77–3.72 (m, 1H), 3.61–3.59 (m, 2H), 3.44–3.39 (m, 2H), 3.04 (app t, *J* = 4.0 Hz, 4H), 2.42 (app t, *J* = 4.4 Hz, 4H), 2.20 (s, 3H), 1.96–1.78 (m, 3H), 1.57–1.49 (m, 1H). LC–MS (ESI+): *m/z* 539.22118 $(M + H)^+$. HRMS (ESI+): *m/z* calcd for $C_{27}H_{31}ClN_7O_2$ (M + H) 540.2284, found 540.2283.

N^2-[4-(4-Methylpiperazin-1-yl)phenyl]-*N*^{4}-[(tetrahydrofuran-2-yl)methyl]pyrimidine-2,4-diamine [(±)-21]

2-Chloro-*N*-((tetrahydrofuran-2-yl)methyl)pyrimidin-4-amine (0.150 g, 0.0.70 mmol) and 4-(4-methylpiperazin-1-yl)aniline (0.148 g, 0.0.77 mmol) were mixed in a microwave vial with HCl (140 μL of a 4 M solution in dioxane). The solvent 2-methoxyethanol (4.00 mL) was added to the mixture, and the resulting solution was heated at 110 °C for 16 h. The resulting solution was concentrated, and the product was partitioned between $CHCl_3$ and saturated aqueous $NaHCO_3$. The organic phase was then dried (Na_2SO_4), filtered, and concentrated under reduced pressure. The resulting solid was slurried twice with dichloromethane and hexane, filtered, and dried under reduced pressure to yield **21** as a dark brown solid (0.108 g, 58%). Mp: 212 °C dec. HPLC: 99.9% [t_R = 9.36 min, 55% CH_3OH in water (0.1% TFA), 20 min]. ^{1}H NMR (400 MHz, DMSO) δ 8.64 (s, 1H), 7.71 (br s, 1H), 7.56 (d, *J* = 9.2 Hz, 2H), 7.16 (br s, 1H), 6.79 (d, *J* = 9.2, 2H), 5.88 (d, *J* = 5.6 Hz, 1H), 3.99–3.93 (m, 1H), 3.77–3.74 (m, 1H), 3.64–3.58 (m, 2H), 3.00 (t, *J* = 5.2 Hz, 4H), 2.42 (t, *J* = 4.8 Hz, 4H), 2.19 (s, 3H), 1.92–1.77 (m, 3H), 1.57–1.50 (m, 1H). LC–MS (ESI+): *m/z* 369.23246 $(M + H)^+$. HRMS (ESI+): *m/z* calcd for $C_{20}H_{28}N_6O$ (M + H) 369.2397, found 369.2407.

4-(4-{4-[[5-((2-Chloro-6-fluorophenyl)carbamoyl)-4-(((tetrahydrofuran-2-yl)methyl)amino)pyrimidin-2-yl]amino]phenyl}piperazin-1-yl)-4-oxobutanoic Acid [(±)-22]

To a suspension of **9m** (0.096 g, 0.15 mmol) in chloroform (2 mL) under an inert atmosphere was added DIPEA (0.194 g, 1.5 mmol). The mixture became a clear solution and was cooled to 0 °C. Succinic anhydride (0.015 g, 0.15 mmol) was added slowly, and the reaction mixture was warmed to rt and stirred for 1 h. The solvent was removed under reduced pressure. The resulting residue was sonicated in water (5 mL), filtered, washed with water (3 mL), and dried under vacuum to afford the title compound **22** as a light green solid (0.084 g, 89%). Mp: 189 °C dec. HPLC: 99.0% [t_R = 3.71 min, 60% CH_3OH in 0.1% TFA/water, 20 min]. ^{1}H NMR (400 MHz, DMSO-d_6): δ 12.03 (s, 1H, disappeared on D_2O shake), 9.84 (s, 1H, disappeared on D_2O shake), 9.51 (s, 1H, disappeared on D_2O shake), 8.85 (s, 1H, disappeared on D_2O shake), 8.73 (s, 1H), 7.61 (d, *J* = 8.8 Hz, 2H), 7.43–7.30 (m, 3H), 6.90 (d, *J* = 8.8 Hz, 2H), 4.03–3.97 (m, 1H), 3.75–3.71 (m, 1H), 3.62–3.57 (m, 6H), 3.44–3.39 (m, 1H), 3.07 (br t, 2H), 3.00 (br t, 2H), 2.56 (t, *J* = 6.4 Hz, 2H), 2.42 (t, *J* = 5.6 Hz, 2H), 1.96–1.89 (m, 1H), 1.85–1.78 (m, 2H), 1.57–1.49 (m, 1H). ^{19}F NMR (376 MHz, DMSO-d_6): δ –116.16 to –116.19 (m). LC–MS (ESI+): *m/z* 626.22; $(M + H)^+$. HRMS (ESI+): *m/z* calcd for $C_{30}H_{34}ClFN_7O_5$ (M + H) 626.2289, found 626.2289.

Plasma Stabilities of (*R*)-9b and (*S*)-9b

The in vitro human plasma stabilities of compounds (*R*)-**9b** and (*S*)-**9b** were evaluated using HPLC analysis in a time-course experiment for up to 24 h.

A compound [(*R*)-**9a**, (*S*)-**9a**, procaine, and procainamide, 5 μL of 10 mM stock solutions in DMSO] was added to human plasma (195 μL), and a clear solution was obtained. This mixture was incubated at 37 °C for 0 min, 15 min, 30 min, 1 h, 2 h, 4 h, 8 h, and 24 h. After the incubation time MeOH (400 μL) was added to the sample vial. A white precipitate was observed, and the mixture was centrifuged for 15 min. An aliquot (400 μL) of the supernatant was removed from the mixture, and 60 μL was injected for analysis by HPLC. The percentage of the compound remaining vs time showed the stability of each compound in human plasma. Procaine and procainamide were run as unstable and stable standards, respectively.

Supplementary Material

Refer to Web version on PubMed Central for supplementary material.

ACKNOWLEDGMENTS

This work is supported in part by a Department of Defense grant (W81XWH-12-1-0248) to K.M. and by a National Cancer Institute, NIH/NCI, grant (1R01CA135328) and Department of Defense grants (W81XWH-14-1-0002 and W81XWH-14-1-0003) to N.P.M. This work has been supported in part by the Chemical Biology Core Facility (Chemistry Unit for synthesis and analytical chemistry support and Structural Biology Unit for production and purification of ACK1) at the H. Lee Moffitt Cancer Center & Research Institute, an NCI-designated Comprehensive Cancer Center (Grant P30-CA076292).

ABBREVIATIONS USED

ACK1	activated CDC42-associated kinase 1
AR	androgen receptor
CRPC	castration-resistant prostate cancer
DIPEA	*N*,*N*-diisopropylethylamine

REFERENCES

1. Mahajan K, Mahajan NP. ACK1 tyrosine kinase: targeted inhibition to block cancer cell proliferation. Cancer Lett. 2013; 338:185–192. [PubMed: 23597703]
2. Mahajan K, Mahajan NP. ACK1/TNK2 tyrosine kinase: molecular signaling and evolving role in cancers. Oncogene. 2014 DOI: 10.1038/onc.2014.350.
3. Mahajan K, Mahajan NP. Shepherding AKT and androgen receptor by Ack1 tyrosine kinase. J. Cell. Physiol. 2010; 224:327–333. [PubMed: 20432460]
4. Mahajan NP, Liu Y, Majumder S, Warren MR, Parker CE, Mohler JL, Earp HS, Whang YE. Activated Cdc42-associated kinase Ack1 promotes prostate cancer progression via androgen receptor tyrosine phosphorylation. Proc. Natl. Acad. Sci. U.S.A. 2007; 104:8438–8443. [PubMed: 17494760]
5. Mahajan K, Coppola D, Rawal B, Chen YA, Lawrence HR, Engelman RW, Lawrence NJ, Mahajan NP. Ack1-mediated androgen receptor phosphorylation modulates radiation resistance in castration-resistant prostate cancer. J. Biol. Chem. 2012; 287:22112–22122. [PubMed: 22566699]
6. Aqeilan RI, Croce CM. WWOX in biological control and tumorigenesis. J. Cell. Physiol. 2007; 212:307–310. [PubMed: 17458891]
7. Mahajan NP, Whang YE, Mohler JL, Earp HS. Activated tyrosine kinase Ack1 promotes prostate tumorigenesis: role of Ack1 in polyubiquitination of tumor suppressor Wwox. Cancer Res. 2005; 65:10514–10523. [PubMed: 16288044]

8. Mahajan K, Coppola D, Challa S, Fang B, Chen YA, Zhu W, Lopez AS, Koomen J, Engelman RW, Rivera C, Muraoka-Cook RS, Cheng JQ, Schonbrunn E, Sebti SM, Earp HS, Mahajan NP. Ack1 mediated AKT/PKB tyrosine 176 phosphor-ylation regulates its activation. PLoS One. 2010; 5:e9646. [PubMed: 20333297]

9. Franke TF, Yang SI, Chan TO, Datta K, Kazlauskas A, Morrison DK, Kaplan DR, Tsichlis PN. The protein kinase encoded by the Akt proto-oncogene is a target of the PDGF-activated phosphatidylinositol 3-kinase. Cell. 1995; 81:727–736. [PubMed: 7774014]

10. Burgering BM, Coffer PJ. Protein kinase B (c-Akt) in phosphatidylinositol-3-OH kinase signal transduction. Nature. 1995; 376:599–602. [PubMed: 7637810]

11. Manning BD, Cantley LC. AKT/PKB signaling: navigating downstream. Cell. 2007; 129:1261–1274. [PubMed: 17604717]

12. Mahajan K, Coppola D, Chen YA, Zhu W, Lawrence HR, Lawrence NJ, Mahajan NP. Ack1 tyrosine kinase activation correlates with pancreatic cancer progression. Am. J. Pathol. 2012; 180:1386–1393. [PubMed: 22322295]

13. Mahajan K, Lawrence HR, Lawrence NJ, Mahajan NP. ACK1 tyrosine kinase interacts with histone demethylase KDM3A to regulate the mammary tumor oncogene HOXA1. J. Biol. Chem. 2014; 289:28179–28191. [PubMed: 25148682]

14. DiMauro EF, Newcomb J, Nunes JJ, Bemis JE, Boucher C, Buchanan JL, Buckner WH, Cheng A, Faust T, Hsieh F, Huang X, Lee JH, Marshall TL, Martin MW, McGowan DC, Schneider S, Turci SM, White RD, Zhu X. Discovery of 4-amino-5,6-biaryl-furo[2,3-d]pyrimidines as inhibitors of Lck: development of an expedient and divergent synthetic route and preliminary SAR. Bioorg. Med. Chem. Lett. 2007; 17:2305–2309. [PubMed: 17280833]

15. Martin MW, Newcomb J, Nunes JJ, Bemis JE, McGowan DC, White RD, Buchanan JL, DiMauro EF, Boucher C, Faust T, Hsieh F, Huang X, Lee JH, Schneider S, Turci SM, Zhu X. Discovery of novel 2,3-diarylfuro[2,3-b]pyridin-4-amines as potent and selective inhibitors of Lck: synthesis, SAR, and pharmacokinetic properties. Bioorg. Med. Chem. Lett. 2007; 17:2299–3304. [PubMed: 17276681]

16. Mahajan K, Challa S, Coppola D, Lawrence H, Luo Y, Gevariya H, Zhu W, Chen YA, Lawrence NJ, Mahajan NP. Effect of Ack1 tyrosine kinase inhibitor on ligand-independent androgen receptor activity. Prostate. 2010; 70:1274–1285. [PubMed: 20623637]

17. Kopecky DJ, Hao X, Chen Y, Fu J, Jiao X, Jaen JC, Cardozo MG, Liu J, Wang Z, Walker NP, Wesche H, Li S, Farrelly E, Xiao SH, Kayser F. Identification and optimization of N3,N6-diaryl-1H-pyrazolo[3,4-d]pyrimidine-3,6-diamines as a novel class of ACK1 inhibitors. Bioorg. Med. Chem. Lett. 2008; 18:6352–6356. [PubMed: 18993068]

18. Miduturu CV, Deng X, Kwiatkowski N, Yang W, Brault L, Filippakopoulos P, Chung E, Yang Q, Schwaller J, Knapp S, King RW, Lee JD, Herrgard S, Zarrinkar P, Gray NS. High-throughput kinase profiling: a more efficient approach toward the discovery of new kinase inhibitors. Chem. Biol. 2011; 18:868–879. [PubMed: 21802008]

19. Jin M, Wang J, Kleinberg A, Kadalbajoo M, Siu KW, Cooke A, Bittner MA, Yao Y, Thelemann A, Ji Q, Bhagwat S, Mulvihill KM, Rechka JA, Pachter JA, Crew AP, Epstein D, Mulvihill MJ. Discovery of potent, selective and orally bioavailable imidazo[1,5-a]pyrazine derived ACK1 inhibitors. Bioorg. Med. Chem. Lett. 2013; 23:979–984. [PubMed: 23317569]

20. Golas JM, Arndt K, Etienne C, Lucas J, Nardin D, Gibbons J, Frost P, Ye F, Boschelli DH, Boschelli F. SKI-606, a 4-anilino-3-quinolinecarbonitrile dual inhibitor of Src and Abl kinases, is a potent antiproliferative agent against chronic myelogenous leukemia cells in culture and causes regression of K562 xenografts in nude mice. Cancer Res. 2003; 63:375–381. [PubMed: 12543790]

21. Remsing Rix LL, Rix U, Colinge J, Hantschel O, Bennett KL, Stranzl T, Muller A, Baumgartner C, Valent P, Augustin M, Till JH, Superti-Furga G. Global target profile of the kinase inhibitor bosutinib in primary chronic myeloid leukemia cells. Leukemia. 2009; 23:477–485. [PubMed: 19039322]

22. Tan DS, Haaland B, Gan JM, Tham SC, Sinha I, Tan EH, Lim KH, Takano A, Krisna SS, Thu MM, Liew HP, Ullrich A, Lim WT, Chua BT. Bosutinib inhibits migration and invasion via ACK1 in KRAS mutant non-small cell lung cancer. Mol. Cancer. 2014; 13:13. [PubMed: 24461128]

23. Carter TA, Wodicka LM, Shah NP, Velasco AM, Fabian MA, Treiber DK, Milanov ZV, Atteridge CE, Biggs WH III, Edeen PT, Floyd M, Ford JM, Grotzfeld RM, Herrgard S, Insko DE, Mehta SA, Patel HK, Pao W, Sawyers CL, Varmus H, Zarrinkar PP, Lockhart DJ. Inhibition of drug-resistant mutants of ABL, KIT, and EGF receptor kinases. Proc. Natl. Acad. Sci. U.S.A. 2005; 102:11011–11016. [PubMed: 16046538]
24. Liu Y, Karaca M, Zhang Z, Gioeli D, Earp HS, Whang YE. Dasatinib inhibits site-specific tyrosine phosphorylation of androgen receptor by Ack1 and Src kinases. Oncogene. 2010; 29:3208–3216. [PubMed: 20383201]
25. Li J, Rix U, Fang B, Bai Y, Edwards A, Colinge J, Bennett KL, Gao J, Song L, Eschrich S, Superti-Furga G, Koomen J, Haura EB. A chemical and phosphoproteomic characterization of dasatinib action in lung cancer. Nat. Chem. Biol. 2010; 6:291–299. [PubMed: 20190765]
26. Galkin AV, Melnick JS, Kim S, Hood TL, Li N, Li L, Xia G, Steensma R, Chopiuk G, Jiang J, Wan Y, Ding P, Liu Y, Sun F, Schultz PG, Gray NS, Warmuth M. Identification of NVP-TAE684, a potent, selective, and efficacious inhibitor of NPMALK. Proc. Natl. Acad. Sci. U.S.A. 2007; 104:270–275. [PubMed: 17185414]
27. Davis MI, Hunt JP, Herrgard S, Ciceri P, Wodicka LM, Pallares G, Hocker M, Treiber DK, Zarrinkar PP. Comprehensive analysis of kinase inhibitor selectivity. Nat. Biotechnol. 2011; 29:1046–1051. [PubMed: 22037378]
28. Metz JT, Johnson EF, Soni NB, Merta PJ, Kifle L, Hajduk PJ. Navigating the kinome. Nat. Chem. Biol. 2011; 7:200–202. [PubMed: 21336281]
29. Jiao X, Kopecky DJ, Liu J, Jaen JC, Cardozo MG, Sharma R, Walker N, Wesche H, Li S, Farrelly E, Xiao SH, Wang Z, Kayser F. Synthesis and optimization of substituted furo[2,3-d]-pyrimidin-4-amines and 7H-pyrrolo[2,3-d]pyrimidin-4-amines as ACK1 inhibitors. Bioorg. Med. Chem. Lett. 2012; 22:6212–6217. [PubMed: 22929232]
30. Bossi RT, Saccardo MB, Ardini E, Menichincheri M, Rusconi L, Magnaghi P, Orsini P, Avanzi N, Borgia AL, Nesi M, Bandiera T, Fogliatto G, Bertrand JA. Crystal structures of anaplastic lymphoma kinase in complex with ATP competitive inhibitors. Biochemistry. 2010; 49:6813–6825. [PubMed: 20695522]
31. Bernhart, C.; Bouaboula, M.; Casellas, P.; Jegham, S.; Arigon, J.; Combet, R.; Hilairet, S.; Fraisse, P. Nicotinamide derivatives, preparation thereof and therapeutic use thereof. 2010. US20100222319A1
32. Martin MP, Zhu JY, Lawrence HR, Pireddu R, Luo Y, Alam R, Ozcan S, Sebti SM, Lawrence NJ, Schonbrunn E. A novel mechanism by which small molecule inhibitors induce the DFG flip in Aurora A. ACS Chem. Biol. 2012; 7:698–706. [PubMed: 22248356]
33. Yang H, Lawrence HR, Kazi A, Gevariya H, Patel R, Luo Y, Rix U, Schonbrunn E, Lawrence NJ, Sebti SM. Dual Aurora A and JAK2 kinase blockade effectively suppresses malignant transformation. Oncotarget. 2014; 5:2947–2961. [PubMed: 24930769]
34. Cooper KD, Walborsky HM. Alkali metals dissolved in optically active solvents. J. Org. Chem. 1981; 46:2110–2116.
35. Jones G, Willett P, Glen RC. Molecular recognition of receptor sites using a genetic algorithm with a description of desolvation. J. Mol. Biol. 1995; 245:43–53. [PubMed: 7823319]
36. Verdonk ML, Cole JC, Hartshorn MJ, Murray CW, Taylor RD. Improved protein–ligand docking using GOLD. Proteins: Struct., Funct., Bioinf. 2003; 52:609–623.
37. Zhang J, Yang PL, Gray NS. Targeting cancer with small molecule kinase inhibitors. Nat. Rev. Cancer. 2009; 9:28–39. [PubMed: 19104514]
38. Hartman, DA. Current Protocols in Pharmacology. Wiley; New York: 2003. Determination of the stability of drugs in plasma.. Chapter 7, Unit 7.6
39. Lawrence HR, Martin MP, Luo Y, Pireddu R, Yang H, Gevariya H, Ozcan S, Zhu JY, Kendig R, Rodriguez M, Elias R, Cheng JQ, Sebti SM, Schonbrunn E, Lawrence NJ. Development of o-chlorophenyl substituted pyrimidines as exceptionally potent aurora kinase inhibitors. J. Med. Chem. 2012; 55:7392–7416. [PubMed: 22803810]
40. Park CH, Choe H, Jang IY, Kwon SY, Latif M, Lee HK, Lee HJ, Yang EH, Yun JI, Chae CH, Cho SY, Choi SU, Ha JD, Jung H, Kim HR, Kim P, Lee CO, Yun CS, Lee K. Novel bis-ortho-alkoxy-para-piperazinesubstituted-2,4-dianilinopyrimidines (KRCA-0008) as potent and selective ALK

inhibitors for anticancer treatment. Bioorg. Med. Chem. Lett. 2013; 23:6192–6196. [PubMed: 24095090]

41. Di L, Kerns EH, Hong Y, Chen H. Development and application of high throughput plasma stability assay for drug discovery. Int. J. Pharm. 2005; 297:110–119. [PubMed: 15876500]
42. Koch-Weser J. Clinical application of the pharmacokinetics of procaine amide. Cardiovasc. Clin. 1974; 6:63–75. [PubMed: 4613464]

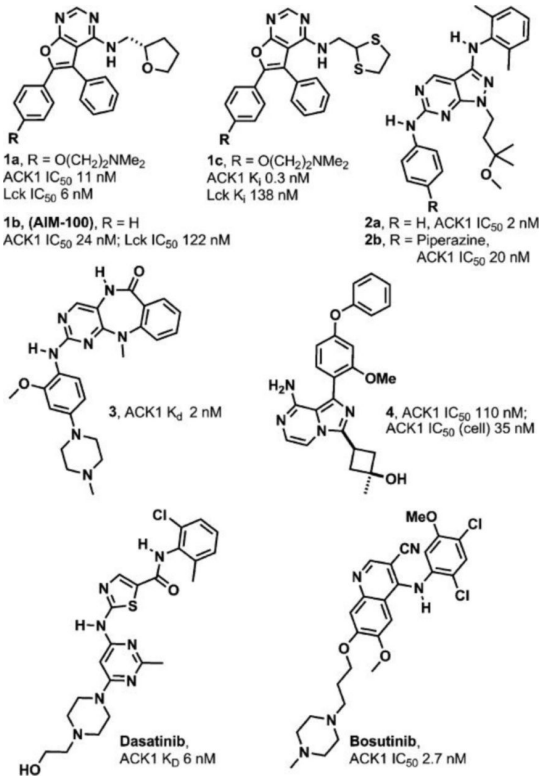

Figure 1.
Structures and activities of representative ACK1 inhibitors.

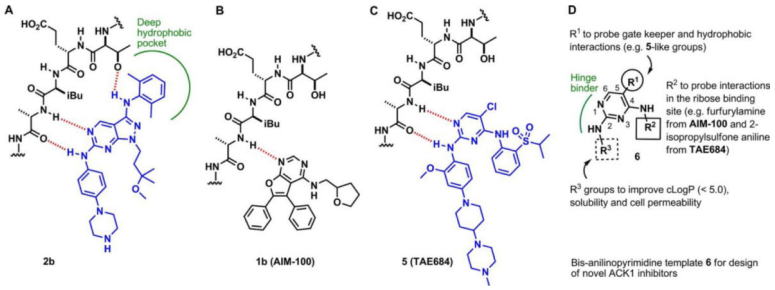

Figure 2.

(A–C) Binding modes of known ACK1 inhibitors to ACK1: (A) compound **2b** taken from its crystal structure with ACK1 (PDB 3EQP), (B) compound **1b** modeled with ACK1, based on similar compounds bound to Lck (PDB 2OF2), and (C) compound **5** (TAE684) modeled with ACK1, based on its crystal structure with ALK (PDB 2XB7). (D) Bisanilinopyrimidine scaffold **6** for design of novel ACK1 inhibitors.

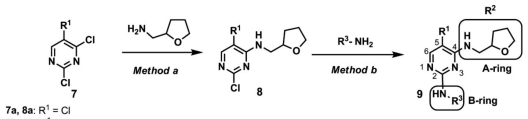

7a, 8a: R^1 = Cl
7b, 8b: R^1 = Br
7c, 8c: R^1 = 2-Chloro-6-fluorocarboxamide
7d, 8d: R^1 = F
7e, 8e: R^1 = Me

Pyrimidines 9a-t

9a: R^1 = Cl, R^3 = 4-(piperazinyl)phenyl
9b: R^1 = Cl, R^3 = (4-methylpiperazinyl)phenyl
9c: R^1 = Cl, R^3 = 4-morpholinophenyl
9d: R^1 = Cl, R^3 = 4-(piperidinyl-methyl)phenyl
9e: R^1 = Cl, R^3 = 1-(4-phenyl)piperidine-4-carboxylic acid
9f: R^1 = Cl, R^3 = 4-(piperidinyl)phenyl
9g: R^1 = Br, R^3 = 2-chloro-4-hydroxyphenyl
9h: R^1 = Br, R^3 = 4-morpholinophenyl
9i: R^1 = Br, R^3 = 4-(piperazinyl)phenyl
9j: R^1 = Br, R^3 = 1-(4-phenyl)piperidine-4-carboxylic acid
9k: R^1 = Br, R^3 = 4-(piperidinyl)phenyl
9l: R^1 = 2-Chloro-6-fluorocarboxamide, R^3 = 1-(4-phenyl)piperidine-4-carboxylic acid
9m: R^1 = 2-Chloro-6-fluorocarboxamide, R^3 = 4-(piperazinyl)phenyl
9n: R^1 = 2-Chloro-6-fluorocarboxamide, R^3 = 4-morpholinophenyl
9o: R^1 = 2-Chloro-6-fluorocarboxamide, R^3 = 4-(piperidinyl)phenyl
9p: R^1 = 2-Chloro-6-fluorocarboxamide, R^3 = 3-fluoro-4-hydroxyphenyl
9q: R^1 = 2-Chloro-6-fluorocarboxamide, R^3 = 4-methoxyphenyl
9r: R^1 = 2-Chloro-6-fluorocarboxamide, R^3 = 4-hydroxyphenyl
9s: R^1 = F, R^3 = 3-fluoro-4-hydroxyphenyl
9t: R^1 = Me, R^3 = 3-fluoro-4-hydroxyphenyl

[a]Method a: (±)-tetrahydrofurfurylamine, Et_3N, MeOH, 0 °C to rt, 2 h. Method b: cat. HCl (4 M) in dioxane, 2-methoxyethanol or ethanol or dioxane, sealed tube, 80−180 °C, 20−30 min, aq $NaHCO_3$ workup.

Scheme 1.

Design and Synthesis of Bisanilinopyrimidine Derivatives 9a–t with a (±)-Tetrahydrofurfurylamine A-Ring[a]

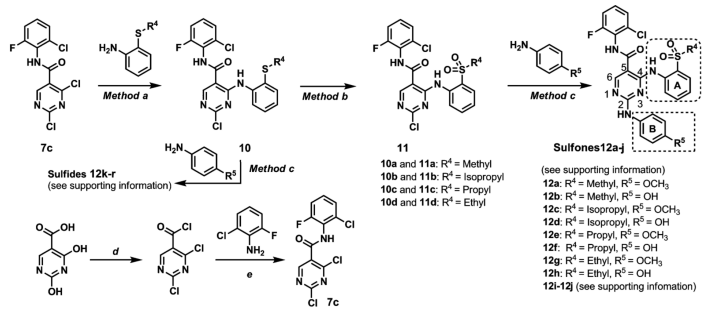

[a]See the Supporting Information. Method a: DIPEA, THF, 120 °C, 1 h, 77−90%. Method b: *m*CPBA, EtOAc, 0 °C to rt, 2 h, 70−96%. Method c: cat. HCl (4 M) in dioxane, microwave heating 180 °C, 30 min, 68−97%. Method d: $POCl_3$, 0 °C, PCl_5, 16 h, 99%. Method e: THF, 15 h, 75%.

Scheme 2.

Design and Synthesis of Bisanilinopyrimidines with Sulfone-Substituted and Sulfide A-Rings[a]

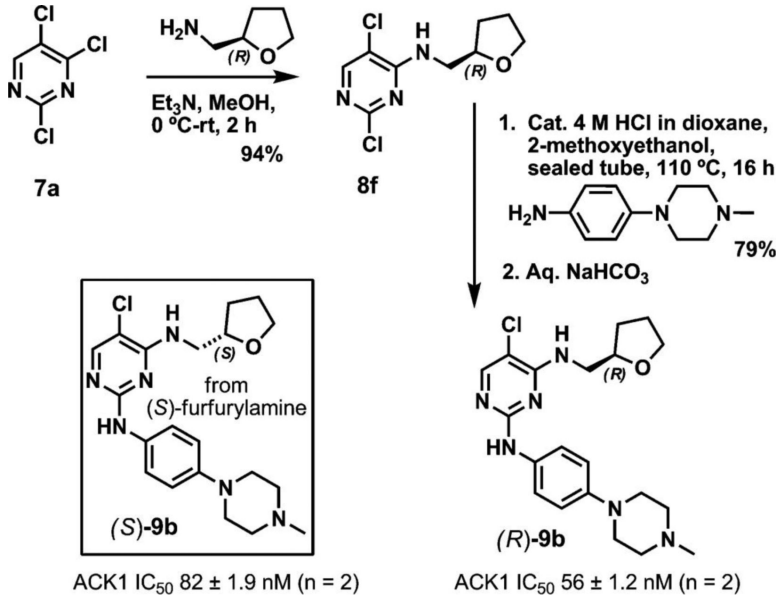

Scheme 3.

Synthesis of (*R*)-9b and (*S*)-9b as ACK1 Inhibitors

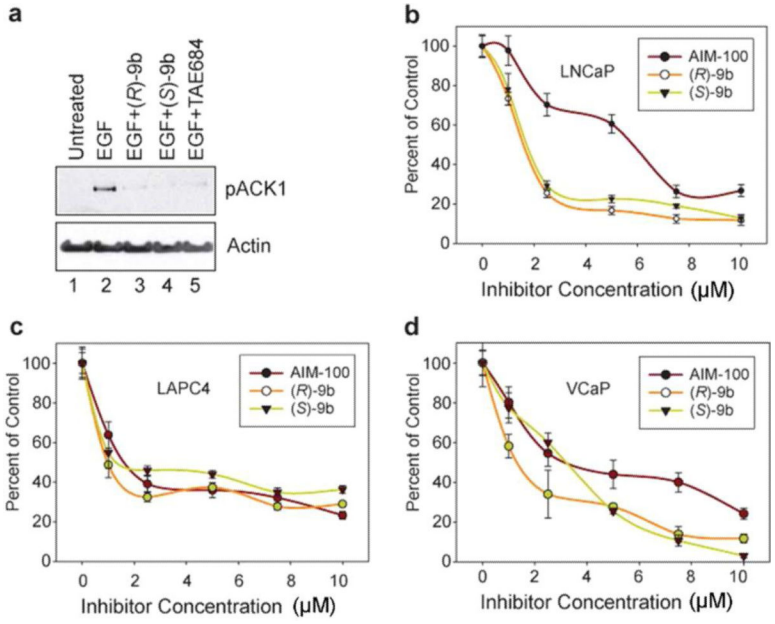

Figure 3.

Effect of ACK1 inhibitors in prostate cancer cells: (a) inhibition of ACK1 autophosphorylation in LAPC4 cells treated with 5 μM (*R*)-**9b** and (*S*)-**9b**; inhibition of (b) LNCaP, (c) LAPC4, and (d) VCaP cell growth by AIM-100, (*R*)-**9b**, and (*S*)-**9b**.

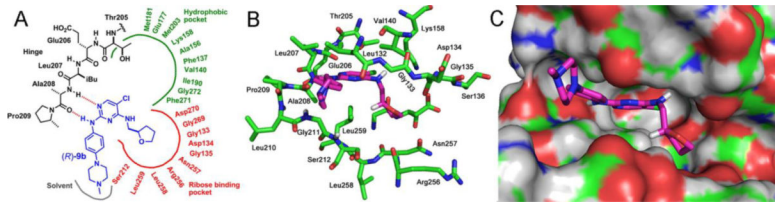

Figure 4.

(A) Schematic representation of compound (*R*)-**9b** (blue) docked to ACK1 (PDB 4EWH), showing the ACK1 amino acid residues in the hinge (black), hydrophobic pocket (green), and ATP-ribose binding pocket (red). (B) Stick model of (*R*)-**9b** (cyan) docked to ACK1 (PDB 4EWH), showing important ACK1 amino acid residues. (C) Surface model of (*R*)-**9b** (cyan) docked to the ATP binding site of ACK1. The surface is colored according to atom type (carbon, green; hydrogen, gray; oxygen, red; nitrogen, blue). The images in panels B and C were rendered using Pymol.

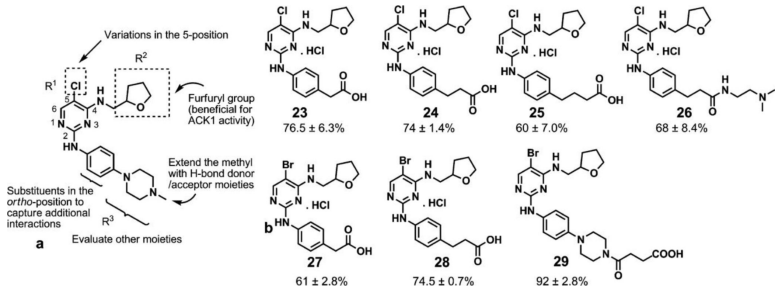

Figure 5.

(a) SAR overview. (b) Compounds with an extended carboxylic acid tether as ACK1 inhibitors (inhibition (%) at 10 μM in ELISA is shown).

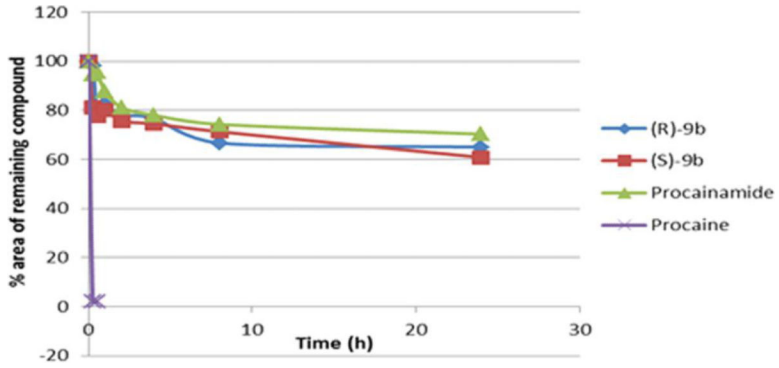

Figure 6.

Plasma stabilities of (*R*)-**9b**, (*S*)-**9b**, procainamide, and procaine using HPLC: area of the peak (*y*-axis) plotted against the time (*x*-axis). Procainamide is reported as stable and procaine unstable in human plasma.[41,42]

Table 1

SAR and in Vitro Inhibitory Activities of Derivatives 9a–t and Related Compounds[b]

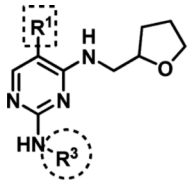

Entry	Compound ID	R^1	R^3	% Inhibition @ 10 μM[a] (ELISA)	IC_{50} (^{33}P Hotspot assay)
1	9t	F	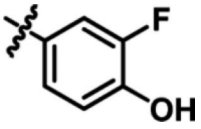	41 ± 6.3	ND
2	9u	CH_3	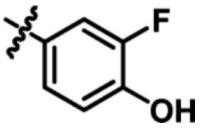	49 ± 2.8	ND
3	13	Br	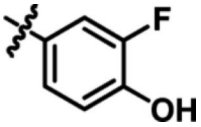	76 ± 14	299 nM
4	14	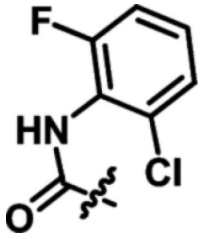	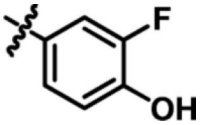	66 ± 1.5	ND
5	15	Cl	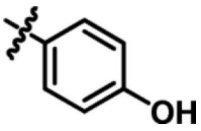	65 ± 10.6	ND
6	16	Br	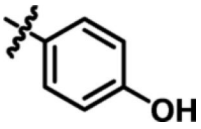	83 ± 2.8	164 nM

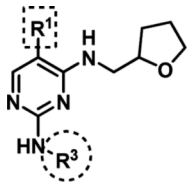

Entry	Compound ID	R^1	R^3	% Inhibition @ 10 μM[a] (ELISA)	IC_{50} (^{33}P Hotspot assay)
7	9r	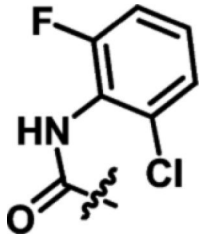	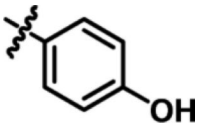	85 ± 0.2	54.4 nM
8	17	Br	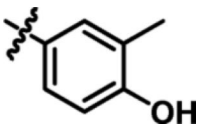	75.5 ± 20	99 nM
9	18	Br	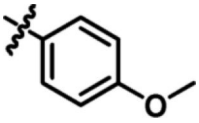	67 ± 0.2	ND
10	9q	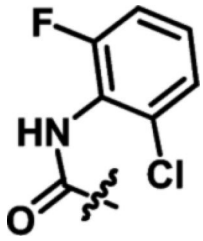	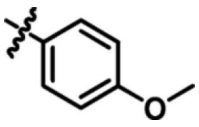	68 ± 10	ND
11	9c	Cl	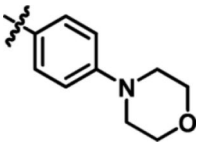	89 ± 1.4	67.5 nM
12	9h	Br	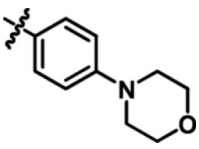	89 ± 1.4	106 nM

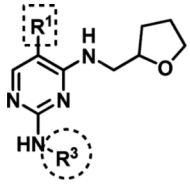

Entry	Compound ID	R^1	R^3	% Inhibition @ 10 μM[a] (ELISA)	IC_{50} (^{33}P Hotspot assay)
13	9n	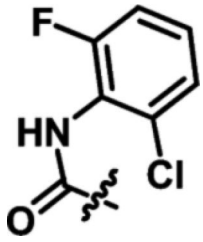	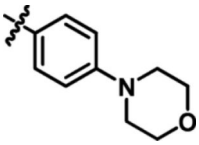	82 ± 7.7	47.7 nM
14	9a	Cl	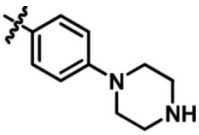	82 ± 12.7	81.3 nM
15	9i	Br	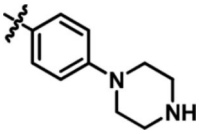	85.5 ± 0.70	94.7 nM
16	9m	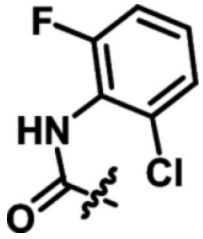	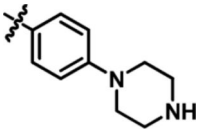	89.5 ± 2.1	33.2 nM
17	9b	Cl	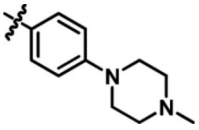	90.5 ± 0.70	54.4 nM
18	19	Br	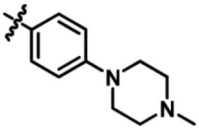	93 ± 3	48.0 nM

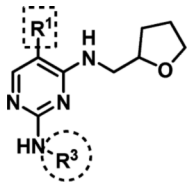

Entry	Compound ID	R^1	R^3	% Inhibition @ 10 μM[a] (ELISA)	IC_{50} (^{33}P Hotspot assay)
19	20	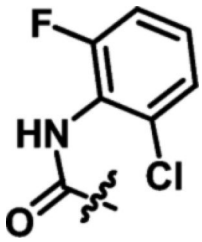	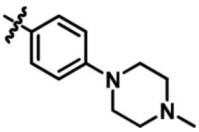	97 ± 3	48.3 nM
20	21	H	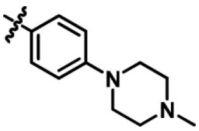	16 ± 4.2	ND
21	9f	Cl	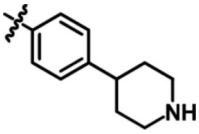	79.5 ± 0.70	231 nM
22	9k	Br	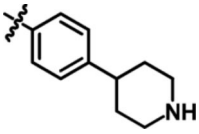	84.5 ± 0.70	169 nM
23	9o	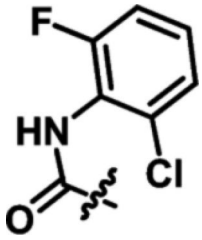	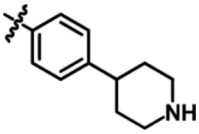	97	53.3 nM
24	9e	Cl	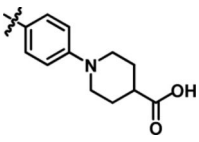	93 ± 5.1	85 nM

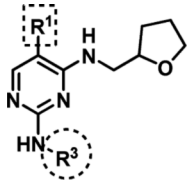

Entry	Compound ID	R^1	R^3	% Inhibition @ 10 μM[a] (ELISA)	IC_{50} (^{33}P Hotspot assay)
25	9j	Br	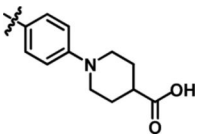	85 ± 2.8	ND
26	9s	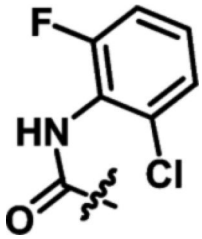	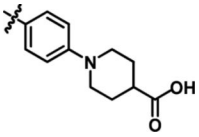	98	34.2 nM
27	22	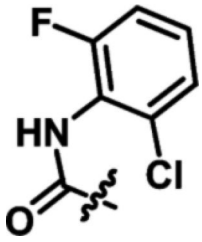	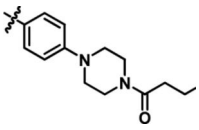	89 ± 5.6	28.4 nM

IC_{50} values were determined for compounds that showed >80% inhibition in the ELISA assay

[a] Inhibition (%) values are given as the average of three or more determinations.

[b] ND = not determined.

Table 2

In Vivo Inhibitory Activities of Derivatives of 9 from Scheme 1[a]

compd ID	inhibition (%) of ACK1 Tyr phosphorylation at 5 μM, 16 h	compd ID	inhibition (%) of ACK1 Tyr phosphorylation at 5 μM, 16 h
DMSO	0	methyl ester of (±)-**9e**	(–12.0)
(±)-**9b**	65.3	(±)-**9e**	1.2
(±)-**9r**	34.3	(*R*)-**9e**	83.3
(±)-**9m**	36.7	(*S*)-**9c**	39.3
22 (Table1)	74.5	(*R*)-**9b**	93.5
(±)-**9i**	58.3	(*S*)-**9b**	78.7
(*R*)-**9c**	(–22.1)	**23** (Table1)	74.5
(±)-**9n**	(–32.6)	(±)-**9l**	8.56
(±)-**9l**	(–49.3)	TAE684 (Figure 2)	86.8
AIM-100 (Figure 1)	70.0		

[a]Inhibition (%) of ACK1 Tyr284 phosphorylation assessed by immunoblotting in LAPC4 cells. Negative values represent increased Tyr phosphorylation (or enhanced kinase activity).

Table 3

Kinase Profiling of (*R*)-9b (Reaction Biology, HotSpot Assay)

kinase	inhibition (%) of 9b at 1 μM[a]	std dev	kinase	inhibition (%) of 9b at 1 μM[a]	std dev
ABL1	82.8	0.5	IR	46.6	1.8
ACK1	99.8	0.3	JAK2	98.6	0.4
AKT1	4.7	2.4	KDR/VEGFR2	67.3	0.0
ALK	86.0	0.1	LCK	87.7	0.0
AXL	75.9	0.0	mTOR/FRAP1	–5.6	1.8
BTK	45.1	0.2	p70S6K/RPS6KB1	24.1	1.3
c-MET	23.1	0.5	PDGFRa	42.7	0.4
CHK1	84.8	0.3	PIM1	3.6	0.2
COT1/MAP3K8	–7.7	0.1	RAF1	–0.8	3.0
CSK	26.3	0.1	ROS/ROS1	84.2	0.2
EGFR	–2.8	3.8	c-Src	71.3	*b*
EPHA2	31.9	0.1	SGK1	26.0	0.1
ERBB2/HER2	–1.1	1.6	TBK1	71.8	0.5
ERK1	1.9	0.2	TIE2/TEK	32.0	0.3
FGFR1	86.4	0.1	TRKA	63.2	0.0
FRK/PTK5	41.3	0.0	TYK2	98.9	0.2
GSK3a	5.1	0.7	WEE1	12.4	0.8
IKKa/CHUK	0.4	0.8			

[a] ATP was used at 10 μM.

[b] Estimated from dose response.